University of Utrecht
Debye Institute for Nanomaterials Science
Group of Inorganic Chemistry and Catalysis

Master Thesis

Elucidation of the Oligomerization and Polymerization Mechanisms of Ethylene over the SiO_2-Supported Chromium Catalyst

Author:
Ilse K. van Ravenhorst

Supervisors:
Dimitrije Cicmil
Dr. Pieter Bruijnincx
Prof. Dr. Ir. Bert Weckhuysen

August 27, 2015

In cooperation with:

Total Research And Technology Feluy

Abstract

Although extensive research has been done in the past decades upon revealing the mechanism behind the polymerization over the Phillips silica-supported chromium catalyst (Cr/SiO_2), the polymerization without an activator is still mysterious. With this research, we wish to provide more insight in the mechanism of oligomerization and polymerization of ethylene via *in-situ* Diffuse Reflectance Infrared Fourier Transform Spectroscopy (DRIFTS), *in-situ* Ultraviolet-Visible-Near Infrared Diffuse Reflectance Spectroscopy (UV-Vis-NIR DRS) and Gas Chromatography-Mass Spectrometry (GC-MS).

Besides ethylene being polymerized, it was also oligomerized *in-situ* with a distribution of olefins and paraffins highly dependent on the catalyst composition, as it is shown that addition of Ti is inhibiting trimerization in favor of dimerization. Furthermore, the TEAl cocatalyst highly promotes both polymerization and oligomerization. H_2 reduces the catalyst and leads to less olefins being formed. Increase of Ti loading in the catalyst causes a decrease of olefin selectivity. Furthermore, two different mechanisms are responsible for the polymerization and oligomerization process, *i.e.* Cossee-Arlman and metallacycle respectively.

With this insight, it is possible to tailor the type of branching, by olefins, in the polyethylene chains by altering the Ti loading and its spatial distribution in the Phillips catalyst.

Table of Contents

List of Figures

List of Tables

Chapter 1

Introduction

1.1 Polymers and Polyolefins

Polymers are macromolecules consisting of a large number of repeating subunits, called monomers, joined by the same type of linkage. Polymers were defined by Hermann Staudinger, a German chemist, in the 1920's. [1] They range from natural bio-polymers, DNA and proteins, to familiar synthetic plastics (polyolefins), polyvinyl chloride (PVC) and polystyrene. Polymers are of great interest in science, due to a broad range of unique properties, including toughness, visco-elasticity, and their tendency to form glasses and semi-crystalline structures rather than crystals. The applications of polymers are, *e.g.*, in fibers, adhesives, resistant paints and plastics. Most of the polymers are made from olefins/alkenes (linear α-olefins (LAO's)), unsaturated chemical compounds containing at least one carbon-carbon double bond. Among all of the synthetic polymers/polyolefins, polyethylene (PE) has been and still is by far the most widely used commodity polymer. Today, the production of polyolefins is a multibillion dollar industrial activity and over 60 million tonnes of polyethylene is manufactured each year. [2, 3]

In the past 60 years, numerous polyolefins were produced with different and unique properties. Among the most general polyolefins is high density polyethylene (HDPE), which consists of linear chains without or only a few short branches. Another type of PE is linear low density polyethylene (LLDPE), which consists of linear chains with short branches determined by the co-polymer composition. Finally, low density polyethylene (LDPE), which consists of chains with long side chains as well as short branches. The branching is on about 2% of the carbon atoms in the chain. [4] The principal structural differences of these three classes of polyethylene are illustrated in Figure 1.1. These differences in the polyethylene density and branching type come from the different polymerization procedure, conditions and catalysts used. LDPE is produced by radical combination reactions at high temperature and high pressure (523-573 K and $>$ 50 bar, respectively). The application of LDPE is in film wrap and plastic bags because of their soft and waxy solid properties. The other polyolefins, HDPE and LLDPE, are made by using either homogeneous or heterogeneous catalysts under relatively low temperature and pressure (353-463 K and $<$ 50 bar, respectively). [5] Due to its rigid and translucent solid properties HDPE is used for electrical insulation, bottles and toys. [1] LLDPE has in general the same applications as LDPE, but due to slightly different properties, *i.e.* higher tensile strength and flexibility, it is convenient for making even thinner films. Moreover, LLDPE show a good chemical resistance. Table 1.1 gives an overview of the density differences between the different classes of polyethylene's.

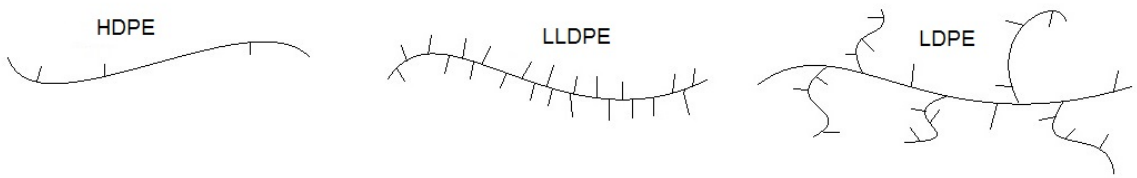

Figure 1.1: Three different classes of polyethylene. [6]

Table 1.1: Density range of three classes of polyethylene's. [7]

Polyethylene	Density (g/cm^3)
HDPE	0.93-0.97 g/cm^3
LDPE	0.91-0.94 g/cm^3
LLDPE	0.91-0.94 g/cm^3

1.2 Olefin Polymerization Catalysts

The discovery of the olefin polymerization catalysts in the early 1950s represents a breakthrough in industrial catalysis. The Phillips silica-supported chromium catalyst (further denoted as Cr/SiO_2 catalyst), discovered by Hogan and Banks at the Phillips Petroleum Company, [8] and the Ziegler-Natta catalyst, discovered by Ziegler and Natta in 1953 [9] are among the most important industrial catalysts for polyethylene production nowadays. Also, the recently commercialized metallocene catalysts are becoming more relevant.

These three types of polymerization catalysts differ in chemical composition, reaction mechanisms and activation of the polymerization.

(i) The *Ziegler-Natta type catalysts* consist of a combination of a transition metal compound and an activator, titanium chloride and an aluminum-alkyl chloride respectively, mostly supported on $MgCl_2$. [5, 10, 11]

(ii) The *metallocene type catalysts* consist of bis-cyclopentadienyl derivatives of either Zr, Hf or Ti in combination with methylaluminoxane (MAO). [5, 10, 11]

(iii) The *Phillips type catalysts* consist of a chromium oxide supported on an amorphous material such as silica or silica-alumina. [5, 10]

The $MgCl_2$-supported Ziegler-Natta catalysts brought a remarkable simplification of polymerization process and led to revolutionary developments for the commercial production of linear PE and isotactic[1] polypropylene (PP). The discovery that the addition of a Lewis base to the $TiCl_4$-$MgCl_2$ binary mixture increased the isotactic content of PP by diminishing the yield of the atactic[2] PP was the second major breakthrough in this field. Nowadays, the majority of heterogeneous Ziegler-Natta catalysts for olefin polymerization are $TiCl_4$-$MgCl_2$-Lewis base ternary mixtures, which become active after addition of the aluminum-alkyl co-catalyst. [12]

Metallocenes are a modern innovation in olefin catalysis research. These "single site" catalysts show only one kind of active sites and are used today mainly for the rapidly increasing production of LLDPE and some special co-polymers. [13] Metallocenes have some advantages over Ziegler-Natta catalysts. For example, in solution polymerization they show higher activity (mainly due to the MAO co-catalyst) and they produce ethylene homo- and co-polymers with narrow molecular weight distribution (MWD). The MWD is responsible for the basic properties of the polymer and it is largely responsible for rheological[3] properties as well. [14] Because metallocenes are a new type of polymerization catalyst, there are several challenges which have to be overcome, *i.e.* maintaining the single-site characterization of metallocenes upon heterogenization, preventing catalyst leaching and eliminating the separate feeding of the MAO co-catalyst. [15]

[1] All substituents are located on the same side of the polymer backbone.

[2] The substituents are placed randomly along the polymer backbone.

[3] Theoretical aspects of rheology are the relation of the flow/deformation behavior of material and its internal structure (*e.g.*, the orientation and elongation of polymer molecules), and the flow/deformation behavior of materials that cannot be described by classical fluid mechanics or elasticity.

In this thesis, only the Phillips catalyst will be extensively discussed, which is known for its specific production of HDPE, as well as some low-density polymers. The success of the Phillips polymerization process originates from its diversity: Phillips catalyst is able to synthesize over 50 different types of HDPE and LLDPE. [16] Furthermore, it does not require the intervention of any activators which is necessary for the other two types of catalysts, a fact that simplifies the catalyst preparation and production process. The latter makes the Phillips catalyst unique as well as a bit mysterious. Although extensive research has been conducted over the past 60 years, the mechanism behind the Phillips catalyst, without an activator, has not yet been revealed. This makes the Phillips catalyst an interesting topic of research.

Another interesting feature of the Phillips catalyst, is the possibility of oligomerization of olefins. [17] Nowadays, olefins are introduced via a separate feed of co-polymer. If the oligomerization process within a single reactor can take place and be influenced, there will be no need of a separate feed, *i.e* 1-hexene or other co-polymers, for the production of LLDPE. This would reduce the possibility of contamination via the feed of co-polymer. This *in-situ* oligomerization will be of economical importance as well, because the price of 1-hexene (9100 €/L [18]) is much higher than that of ethylene (4.85 €/L [18]). As a consequence, the production costs will decrease. This is also discussed in Section 1.6.

1.3 Preparation of the Phillips Catalyst

The preparation of the Phillips catalysts on lab scale is relatively simple and performed by impregnating a chromium compound (usually chromic ester) onto a support material, most commonly a wide pore silica. The material is heated upon calcination in dry air. Around 573 K an esterification reaction between chromic acid and silica occurs, as shown by the * in Figure 1.2(a). Surface hydroxyl groups are consumed while chromium becomes attached to the surface by oxygen linkages (Si-O-Cr). Afterwards, the temperature is slowly increased for the calcination step in O_2 at around 925 K which anchors the chromium sites. This calcination temperature can be varied. For example, increasing the temperature enhances the polymerization activity and especially the termination rate up to 1198 K, from where sintering destroys the silica base. After the calcination phase the chromium species are in the hexavalent state which gives yellow/orange color to the catalyst.

In the industrial preparation procedure, the catalyst is heated first to the esterification temperature followed by calcination at around 950 K. This treatment provides only Cr^{6+} sites. Because Cr^{6+} is toxic and cancerogenic, in industry Cr^{3+} compounds are used which are not or less toxic. After the calcination in oxygen, Cr^{3+} becomes oxidized to Cr^{6+}. Finally, the catalyst is cooled down to room temperature and stored in a glove box under inert environment. [2, 19]

Commercial catalysts usually contain between 0.5-1.0 wt% chromium. Above this concentration, Cr^{6+} converts to the bulk Cr_2O_3 which is an inactive phase for the polymerization. Cutting the concentration in half has little effect on the activity and only a significant decrease in Cr loading will decrease the activity. [16]

If necesary, in order to decrease the polymerization induction time, the Cr^{6+} sites can be pre-reduced to Cr^{2+} by successive reductive treatment at 623 K in CO, followed by removal of CO_2 and absorbed CO at the same temperature, as illustrated in Figure 1.2(b). Cr^{2+} sites are believed to be the active sites for ethylene polymerization. In industry, the catalyst is rarely reduced to Cr^{2+} first, since ethylene acts as a reducing agent during an induction time when chromium is reduced and ethylene is oxidized.

The Phillips catalyst can be promoted by adding up till around 6 wt% Ti. How the titanation effects the polymerization process will be discussed in section 1.6. There are two ways of incorporating

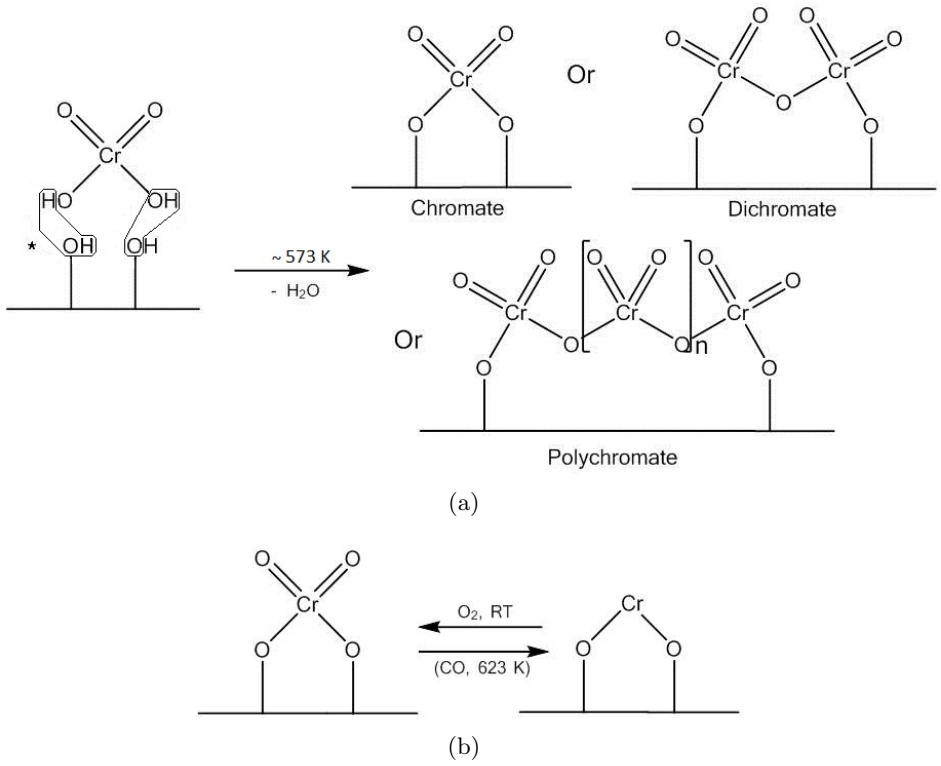

Figure 1.2: (a) Esterification reaction * between chromic acid and alcohol groups on the surface of silica causes anchoring of Cr species in either mono-, di-, or poly-chromate forms. (b) Reduction from Cr^{6+} to Cr^{2+}. [2]

Ti onto the Cr/silica catalyst. With the first method, the silica surface is coated with a layer of Ti by allowing a Ti ester to react with the hydroxyl groups. The second method consists of co-precipitating hydrous Ti along with the silica gel, where the Ti is more evenly distributed through out the catalyst. [16]

1.4 Active Sites for Ethylene Polymerization

After the reduction by the ethylene reactant, CO or other reducing agents, Cr^{2+} is considered to be the main species in the Cr/SiO_2 catalyst. [2] However, the Cr^{2+} sites are not homogeneous. Several spectroscopic and chemical techniques, especially infrared spectroscopy (IR), have shown that it is possible to discriminate between different surface Cr^{2+} species (Figure 1.3). [5, 10–12, 20] Three families of anchored Cr^{2+} ions have been singled out (labeled A, B and C) after chemisorption of CO. They differ in their degree of coordinative unsaturation (A < B < C) and consequently in their propensity to react (A > B > C). [10] The heterogeneity of Cr^{2+} sites is thought to be the basis of the broad molecular weight distribution characteristic of the Phillips catalyst. [7, 16]

1.5 Polymerization Mechanisms

The ability of the Phillips catalyst to polymerize ethylene without the intervention of any activator makes it unique among all of the olefin polymerization catalysts. Although abundant research has been done in the past decades, [2, 11, 12, 16, 21–23] the mechanism of the polymerization without an activator remains mysterious. Several mechanisms are proposed, as illustrated in Figure 1.4.

a) Cossee-Arlman (linear insertion) model

For the Cossee-Arlman mechanism (valid for the Ziegler-Natta catalysts) it is generally accepted which

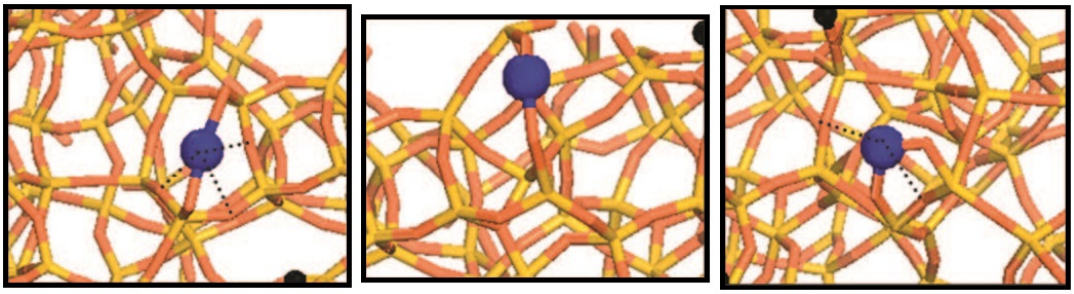

Figure 1.3: Three different Cr^{2+} species characterized by a different coordinative unsaturation. (O, Si, H and Cr atoms are represented by red, yellow, black and blue respectively). [12]

catalytic reactions are involved in the olefin insertion and oligomerization. In this case, the metal active site must possess one alkyl or hydride ligand and an available coordination site. Therefore, the catalyst needs to be activated first, which requires the intervention of an activating agent (MAO in the case of the Ziegler-Natta catalyst) and creation of a vacant site. After the monomer is inserted at the vacant site, the chain propagation starts via a migratory insertion reaction, as is illustrated in Figure 1.4(a). This reaction is repeated numerous times to synthesize the polymer and terminates with a hydrogen β-elimination. [2]

b) Green-Rooney (carbene hydride) model
In this case only one ethylene molecule is coordinated to a chromium site at the time. Via formation of an ethylidene-Cr^{4+} species through a metal-catalyzed transfer of hydrogen between the carbon atoms in ethylene and a metathesis like step the polymer is growing. [2]

c) Metallacycle model
This mechanism avoids additional hydrogen and includes formation of chromacyclopentane by coordinating two ethylene molecules to a chromium site. Larger metallacycles may be formed by further insertions at one of the two chromium-carbon single bonds. The metallacyclic species may propagate as such until termination occurs by hydrogen transfer from one of the β-methylene groups to the opposite α-carbon, thus forming linear polymer chains with one methyl and one vinyl end group as expected. [2] According to Groppo *et al.*, this mechanism is expected to be the mechanism for the *in-situ* oligomerization of ethylene. [21]

In literature, there is a major point of discussion which mechanism should hold for the Phillips catalysts, *i.e.* whether it is the Cossee-Arlman, [22] or the metallacycle mechanism. [21] Overall, there is an agreement that the Green-Rooney mechanism does not give proper answers to the general questions regarding the mechanisms.

If it is indeed true that the Cossee-Arlman mechanism holds for the Phillips catalyst as well, ethylene has to play three important roles simultaneously and/or successively: [2, 11]

(a) As a reduction agent, reducing the chromate species in an oxidation state of 6+ into coordinatively unsaturated active chromium precursor in a lower oxidation state.

(b) As an alkylation agent, alkylating the potential active chromium species resulting in the formation of active sites.

(c) As a propagation agent, acting as a monomer for chain propagation of the active sites.

The difficulties for studying the mechanism of polymerization are mainly derived from the heterogeneity of the active sites, sensitivity to poisons (*i.e.* H_2O, O_2 and organic contamination), low

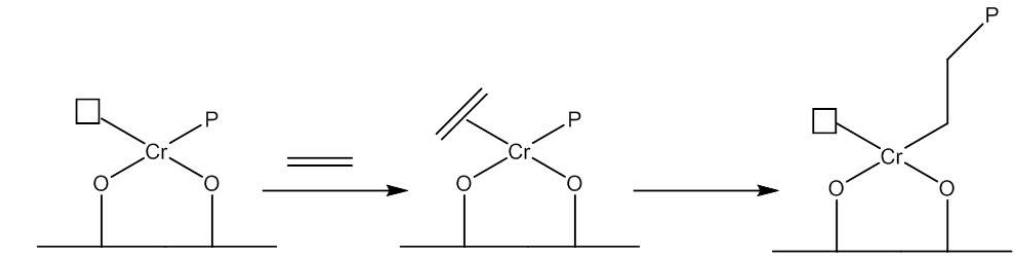

(a) Cossee-Arlman (linear insertion) mechanism

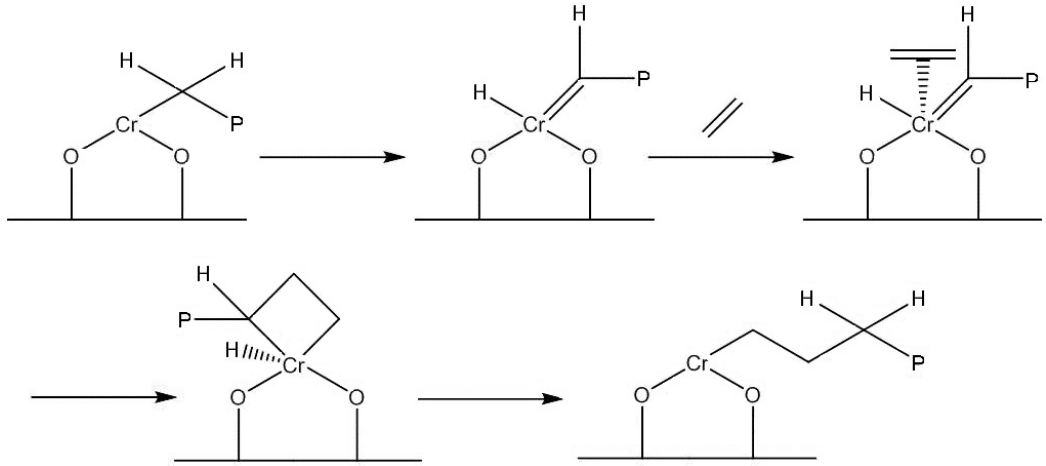

(b) Green-Rooney (carbene hydrides) mechanism

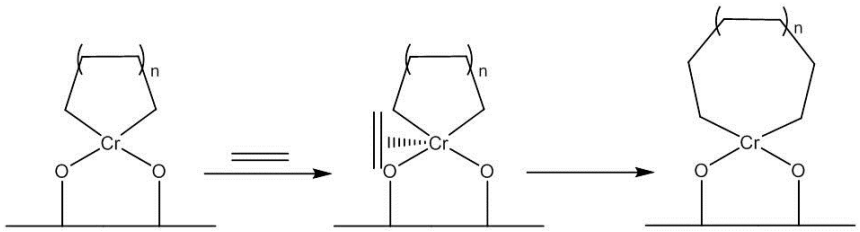

(c) Metallacycle mechanism

Figure 1.4: Different proposed mechanisms of chain growth from the literature. (a) Cossee-Arlman mechanism (migratory insertion of ethylene into the polymer chain) (b) Green-Rooney mechanism (α-hydride shift and metallacyclobutane formation) (c) Metallacycle mechanism (metallacyclopentane formation and growth by ethylene insertion into large-ring metallacycles). [22] P = Polymer chain.

percentage of active sites (0.01-20 % of total Cr), [12, 16] multiple valence states of Cr, the instant encapsulation of active sites by produced polymer and high activity of the Cr species. [23] The low percentage of active Cr species and the ultra-fast polymerization rate makes it difficult to follow the *in-situ* reactions of polymerization with spectroscopic studies. The reaction is too fast to trap intermediates within the few sites.

Additionally, most research reported in the past have been conducted under conditions that are quite far from the real commercial conditions, for instance at a temperature of 298 K and pressures around 1 bar. [5, 22] The actual industrial conditions are in the temperature range of 373-448 K and at pressures of 15-30 bar. An overview of conditions of the polymerization conditions is tabulated in Table 1.2. All these circumstances make it hard to unravel the mystery around the mechanism for polymerization and oligomerization over the Phillips catalyst.

Table 1.2: Polymerization conditions found in the literature.

Reference	Temperature (K)	Pressure (bar)
McGuinness *et al.* [22]	363-413	30
Groppo *et al.* [21]	100-300	<1
Barzan *et al.*[17]	130-300	<1
Groppo *et al.* [24]	308	<1

1.6 Goals

Linear low-density polyethylene (LLDPE) accounts for around one third of the global polyethylene market. [7, 16, 17] Co-monomers, *e.g.* 1-hexene, are used to control the density of polymers and have the beneficial effect on the impact properties of the resin. Co-monomers are usually separately fed into the reactor, which demands additional infrastructure and increases probability of introducing impurities, increasing the risk of catalyst poisoning and decreasing productivity. A single-reactor setup would be less vulnerable to poisoning from different reactant feeders. Furthermore the price of ethylene compared to the price of 1-hexene makes *in-situ* generation of the co-monomer in the reactor highly desirable from a practical and an economical point of view. The whole process would be less expensive if 1-hexene can be produced alongside polymerization.

Bringing the laboratory conditions as close as possible to the industrial conditions in order to synthesize a type of LLDPE is of great scientific and industrial importance. Therefore, the oligomerization of ethylene *in-situ* to 1-hexene and its co-polymerization into the LLDPE under industrial conditions are the main goals for this research. In order to elucidate the exact nature of oligomerization species, different characterization techniques have to be utilized. This work is focused mainly on the *in-situ* Diffuse Reflectance Fourier Transform Infrared Spectroscopy (DRIFTS) and testing of the Phillips polymerization catalyst, supplied by Total Petrochemicals, in a DRIFTS cell at conditions as similar as possible to the industrial conditions (Table 1.3). Also UV-Visible Near Infrared Diffuse Reflectance Spectroscopy (UV-Vis-NIR DRS) will be used to give more inside into the electronic changes within the catalyst and vibrational changes within the forming polymer.

Table 1.3: Specific details about the planned experimental conditions.

Conditions	Planned experiments
Ethylene	45 %
Nitrogen	45 %
Hydrogen	10 %
Co-catalyst (TEAl)	10 μl 1.2 M
Pressure	1 bar
Temperature (K)	373

This involved the development and optimization of a DRIFTS and UV-Vis-NIR DRS setups and their integration with another analysis technique (GC/MS/GC-MS). Several experimental parameters can be varied in order to get a better insight on the oligo/polymerization process:

a) The catalyst preparation (activation temperature and Ti loading).

b) Polymerization conditions (temperature, pressure, co-catalyst, static/flow).

c) Reactant (ethylene/ deuterated ethylene, H_2/D_2, hexene).

a) The catalyst preparation
The catalysts are provided by Total Research and Technology Feluy and differ in Ti loading (0-4 wt% Ti), chromium loading (0.5-1 wt% Cr) and activation temperature (823-1048 K). Ti itself is not a good carrier for Cr^{6+}. However, its presence in small amounts on the Cr/SiO_2 catalyst increases the activity of the catalyst. First by shortening the induction time and second, by allowing higher polymerization rates. [16] It also has a promotional effect on the termination rate. These beneficial effects probably results from a change in the electronic environment on the chromium, which possibly becomes linked to some of the Ti during the calcination, forming Si-O-Ti-O-Cr-O-Si linkages. [16] However, too much Ti may cause sintering, which diminishes the activity of the catalyst. Therefore, Ti is only beneficial when added in small amounts.

b) Polymerization conditions
Temperature, pressure, co-catalyst, H_2/D_2 and static/flow are all variables that can be varied during different experiments. Temperature and pressure influence the reaction rate of the reaction. The temperature is not difficult to be varied, but creating a controlled pressurized atmosphere can be a problem. Furthermore, the co-catalyst (Tri-ethylaluminium (TEAl) mostly) improves the reaction yield, by reducing the catalyst. Furthermore, it would promote the production of olefins. [25]
Furthermore, experiments with a static atmosphere or a continuous flow should be performed as well.

c) Reactants
Experiments with deuterated ethylene/hexene show in their spectra CDx vibrations which shift towards lower energies due to the increase of reduced mass. Also, experiments with D_2 instead of H_2 flow should be performed in order to discover the role of H_2. Is it incorporated in the PE chains or does it go to the oligomers. Furthermore, experiments with hexene should be done to distinguish between the spectrum of ethylene and *in-situ* formed hexene.

In this study we will focus on the effects of activation temperature, Ti-loading, addition of the co-catalyst and hydrogen in order to elucidate *in-situ* oligo- and polymerization of ethylene.

1.7 Experimental Approach

The main techniques used for characterization are Diffuse Reflection Infrared Fourier Transform Spectroscopy (DRIFTS), Ultraviolet-Visible-Near Infrared Diffuse Reflectance Spectroscopy (UV-Vis-NIR DRS), Gas Chromatography (GC) and Gas Chromatography-Mass Spectrometry (GC-MS).

DRIFTS is a type of FT-IR spectroscopy which probes the vibrational modes of molecules. It is an important tool for the characterization of the surface reactivity of gas sensing materials under reactive atmosphere. DRIFTS analysis of powders is conducted by focusing infrared light onto the powder sample and the scattered light is collected and relayed to the IR detector.

UV-Vis-NIR DRS is a valuable technique for the characterization of the catalyst and is based on measurements of electronic and vibrational transitions (combination bands and overtones).

In GC analysis, a volatile liquid or gaseous solute is carried over a stationary phase on the inside of a column or on a solid support by a gaseous mobile phase, called the carrier gas. The solute is rapidly evaporated after injecting into the column and separated by means of interaction with the stationary phase. The carrier gas has an important effect on the analysis time, elution temperature and sensitivity. Which gas is used and what particular role it plays depends also on the detector used. GC provides information about which compounds are present in the mixture and in which ratio.

GC-MS is a very powerful combination for qualitative analysis of volatile liquids or gaseous mixtures. It is build up by a gas chromatograph and a mass spectrometer at the outlet of the GC instrument acting as a detector. Where the gas chromatograph separates the components in the mixture, the mass spectrometer can identify these peaks by creating mass spectra and comparing them with a library of known spectra.

For more extensive details on the techniques employed we refer to Appendix A.

Chapter 2

Experimental Methods

2.1 Catalyst Preparation

All catalyst samples were made and provided by Total Research and Technology Feluy. The catalyst preparation includes the treatment of commercially available Cr/SiO_2 pre-catalyst containing Cr with the following properties: 0.5-1 wt% Cr loading, surface area of ≈500 m^2/g, pore volume of 1.5 ml/g and D50 particle size diameter of ≈ 40 (for all catalyst used except CrTiSi-04) and 70 (CrTiSi-04)μm. The pale white silica was placed in a fluidized bed reactor under N_2 flow and slowly heated to 543 K for dehydration. To make a titanated catalyst, while still under N_2 flow, the pre-catalyst material was surface-titanated with either ≈ 2 or 4 wt% Ti using an organic titanate ester added drop wise to the fluidized bed. The N_2 flow was changed to dry air and the temperature was slowly increased to a maximum of 1048 K. During the oxidation step, the prepared $Cr/Ti/SiO_2$ catalyst color changed to intense orange. After cooling down to the room temperature and switching back to N_2 flow, the activated $Cr/Ti/SiO_2$ catalyst could be obtained under an inert atmosphere, and was then transferred to a glove box for storage and further use. The procedure for the non-titanated catalyst is the same as for the titanated one, however without the step of adding the ester. An overview of different catalysts used is given in Table 2.1.

Table 2.1: Overview of catalysts provided by Total Research and Technology Feluy.

Catalyst	Act. Temp. (K)	Cr^{n+}	wt% Cr	wt% Ti
CrTiSi-04	1048	Cr^{6+}	0.98	4.7
CrSi-01	1048	Cr^{6+}	0.5	0
CrTiSi-02	1048	Cr^{6+}	0.5	2.2
CrTiSi-03	1048	Cr^{6+}	0.5	4

2.2 Infrared Measurements

2.2.1 *In-situ* DRIFT Spectroscopy

All DRIFTS experiments were performed with a Bruker Tensor 37 spectrophotometer with a liquid N_2-cooled MCT detector, in spectral range of 4000-600 cm^{-1} with a 4 cm^{-1} resolution and 32 second scan time. All polymerization reactions were performed at 373 K and 1 bar. All gases were provided by Linde with the following purities: N_2 (99.999 %), H_2 (99.999 %) and C_2H_4 (99.95 %).

The catalyst was loaded into a Praying Mantis High Temperature Reaction Chamber, *i.e.* the DRIFTS cell (Figure 2.1(b)), under inert atmosphere in an argon glove box. In general, the cell was connected to the DRIFTS setup (Figure 2.1(a)), connected to the water pump for the water heating/cooling mantle and the cell heater. In all cases the temperature of the water mantle was set at 353 K and the heater at 383 K. The trace temperature of the line for the gas flows was at all times fixed at 408 K.

Before every measurement the MCT IR detector was filled with liquid N_2 and the signal of the sample was maximized, by adjusting the height of the sampling cup. During the heating of the cell,

several single scans were taken in order to observe any development, while the cell was still closed and under argon. After reaching the right temperature, the N_2 flow was let through the cell ($\approx$ 10 ml/min). Then repeated measurements were started and 10 μl of 1.3 M solution of triethylaluminium (TEAl) in heptanes ($\approx$94 wt% thiethylaluminium, with $\approx$6 wt% predominately tri-n-butylaluminium and less than 0.1 wt% triisobutylaluminium residue, Acros Organics) was injected via the septum for an Al:Cr ratio of 2 (Figure 2.1(a)), in the cases where TEAl was one of the variables. At the point where the TEAl signal nearly changed, the gas bag was connected and the N_2, ethylene and H_2 flows were turned on. In Tables 2.2, 2.3, 2.4 and 2.5 an overview of the samples measured is given for the different catalysts and variables used (abbreviations: NP = No Polymer, LP = Little Polymer and P = Polymer).

In most cases the experiments were performed for about 50 minutes. After that, the gas flows of ethylene and H_2 were set to 0 and the N_2 back to $\pm$ 10 ml/min and the gas bag was removed. After the cell was cooled down, it was cleaned with acetone and stored in an oven at 333 K.

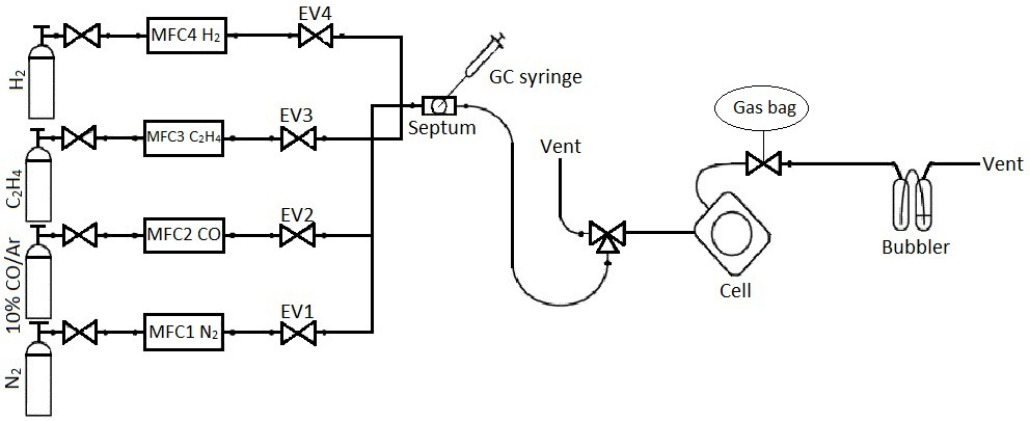

(a)

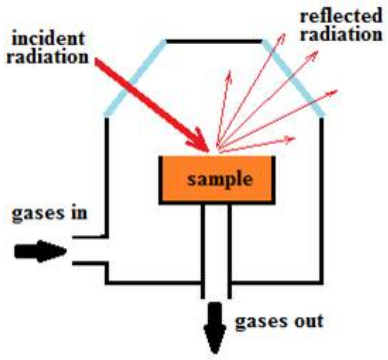

(b)

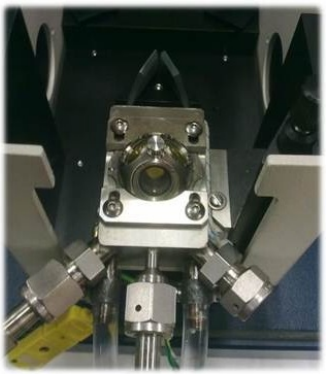

(c)

Figure 2.1: Schematic representation of (a) the setup and (b) the DRIFTS cell. (c) A photo of the DRIFTS cell.

2.2.2 Transmission FT-IR Spectroscopy

Pellets for transmission were prepared by grinding $\pm$ 5 mg of polymer (after polymerization in the DRIFTS cell) with 1 scoop ($\approx$ 0.13 g) of KBr powder. The mixture was then ground to a fine powder and put in the holder. The holder was placed in the press and connected to a vacuum pump. The press was set to 3 tons of weight and held under vacuum for about 30 seconds. The formed pellet was placed

Table 2.2: Overview of experiments for the CrTiSi-04 catalyst (1 wt% Cr, 4.7 wt% Ti).

Catalyst	N_2 (ml/min)	C_4H_4 (ml/min)	H_2 (ml/min)	TEAl (μl)	Comments
CrTiSi-04	9	9	2	10	CHx stretch growing, NP
CrTiSi-04	5	5	-	10	**P**, cell in 120°C oven for 2 weeks
CrTiSi-04	4.5	4.5	1	10	Flush all flows afterwards, NP
CrTiSi-04	4.5	4.5	1	10	**P** → transmission
CrTiSi-04	4.5	4.5	1	-	**LP**
CrTiSi-04	5	5	-	-	CHx stretch but not growing, **LP**
CrTiSi-04	4.5	4.5	1	10	Valves closed during reaction, **P**
CrTiSi-04	4.5	4.5	1	10	1 μl hexene, valves closed during reaction, NP
CrTiSi-04	4.5	4.5	1	10	5 μl hexenes, valves closed during reaction, **P**
CrTiSi-04	4.5	4.5	1	-	CrTiSi-04 pretreated with 1.3 M TEAl, NP

Table 2.3: Overview of experiments for the CrTiSi-03 catalyst (0.5 wt% Cr, 4 wt% Ti).

Catalyst	N_2 (ml/min)	C_4H_4 (ml/min)	H_2 (ml/min)	TEAl (μl)	Comment
CrTiSi-03	5	5	-	-	CHx stretch bands growing and CO at 1700 cm^{-1}, NP
CrTiSi-03	5	5	-	10	Cell was stored in 80 °C oven, NP
CrTiSi-03	5	5	-	-	CHx stretch grow, cell was stored overnight in 120 °C oven, NP

Table 2.4: Overview of experiments for the CrSi-01 catalyst (0.5 wt% Cr, 0 wt% Ti).

Catalyst	N_2 (ml/min)	C_4H_4 (ml/min)	H_2 (ml/min)	TEAl (μl)	Comment
CrSi-01	5	5	-	10	Long induction time, **P** → transmission
CrSi-01	4.5	4.5	1	-	CrSi-01 was pretreated with 1.3 M TEAl, NP
CrSi-01	4.5	4.5	1	1	TEAl syringe was stuck, NP
CrSi-01	4.5	4.5	1	10	**P** → transmission
CrSi-01	5	5	-	10	**P** → transmission

Table 2.5: Overview of blank experiments.

Catalyst	N_2 (ml/min)	C_4H_4 (ml/min)	H_2 (ml/min)	TEAl (μl)	Comment
KBr	4.5	4.5	1	10	Blank experiment
SiO_2	4.5	4.5	1	10	Blank experiment
SiO_2Ti	4.5	4.5	1	10	Blank experiment

into the transmission holder. Measurements were preformed with an aperture of 1.5 mm, spectral resolution of 4 cm^{-1} and 32 scans. The FT-IR data were analyzed with the OPUS Spectroscopy Software.

2.3 *In-situ* UV-Vis-NIR Diffuse Reflectance Spectroscopy

UV-VIS-NIR experiments were performed on a Cary 500 spectrophotometer and in quartz reactors. Approximately 1/3 ($\approx$ 0.3 g) of the quartz reactor was filled with catalyst under inert atmosphere in an argon glove box. The closed cell was than connected to the setup and to the line for the gas flow and a N_2 flow of 9.5 ml/min was let through the cell (Figure 2.2). The cell was placed in front of the UV-Vis-NIR window and covered up with a piece of cloth to protect it from external light. The lines were traced and held at a temperature of 408 K.

The program and details used for the measurements are summarized in Table 2.6.

Table 2.6: Independent UV-Vis and NIR scanning times and ranges.

Region	ave time	Data interval	Scan rate	X-axis (cm^{-1})
UV-Vis	0.033	17.00	30909.092	45000-12500
NIR	0.033	7.096	12901.818	12500-4000

Cycle mode was selected with 60 scans with 0.0 minutes between the different scans for the *in-situ* measurements. Every time ± 0.1 ml of co-catalyst, TEAl, was added in the second cycle for the Al:Cr ratio of 2. After 20-30 minutes the signal of TEAl was almost gone. Then the N_2, H_2 and ethylene flow were switched on according to the experiment (Table 2.7) for 1 hour. Gas was collected in a gas bag for the GC-MS analysis. After the measurements, the cell was disconnected and cleaned with compressed air and acetone, if needed. The catalyst/polymer was saved for further analysis by transmission IR. After cleaning, quarts wool was put into the cell for the next experiment and the cell was placed in a 120 °C oven to dry completely.

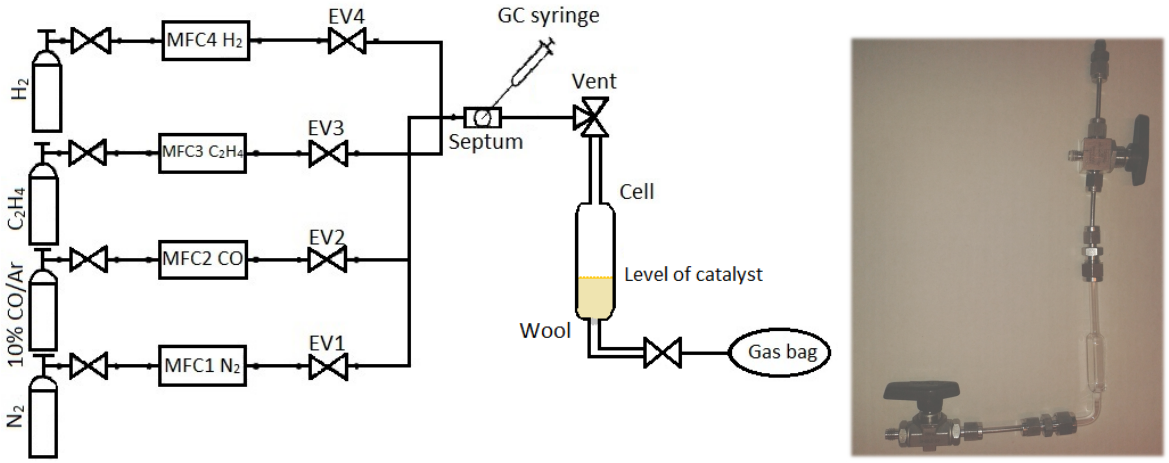

(a) (b)

Figure 2.2: (a) Schematic representation of the UV-Vis-NIR DRS setup and (b) a photo of the cell.

2.4 GC-MS

GC-MS experiments were performed on a GCMS-QP2010 Shimadzu apparatus with a VF-5ms column (30m, 0.25 mm, 0.25 μm, 5% phenyl-methyl/95% dimethyl-polysiloxane). GC experiments were performed on a Varian 430-GC Chromatograph with a column similar to the GC-MS.

With a GC 1 mL gas-tight syringe 1 ml of gas mixture was taken out of the sampled gas from the gasbag, collected during the DRIFTS or UV-Vis-NIR DRS polymerization experiments and injected

Table 2.7: Overview of experiments performed with *in-situ* UV-Vis-NIR DRS.

Catalyst	N_2 (ml/min)	C_4H_4 (ml/min)	H_2 (ml/min)	TEAl (ml)
CrTiSi-04	4.5	4.5	1	0.1
CrTiSi-04	5	5	-	0.1
CrSi-01	4.5	4.5	1	0.1
CrSi-01	5	5	-	0.1
CrTiSi-02	4.5	4.5	1	0.1
CrTiSi-02	5	5	-	0.1
CrTiSi-03	4.5	4.5	1	0.1
CrTiSi-03	5	5	-	0.1
SiO_2	4.5	4.5	1	0.1
SiO_2Ti	4.5	4.5	1	0.1

manually through the septum of the apparatus. All measurements were performed according to the same program and repeated three times. Injector temperature was set at 543 K with column flow of 1 mL/min. FID detector was set at 573 K. After the stabilization time of 1 minute, the temperature of the column was kept constant at 305 K for 15 minutes during the whole analysis. Although the analysis was successful in identifying and separating C6 and C8 hydrocarbons, it was not possible to separate C4 hydrocarbons.

Therefore, in order to achieve good separation on C4 compounds, the analysis of the same samples were performed on another Varian CP-3800 Gas Chromatograph with a Chrompack capillary column with CP-Sil 5 CB stationary phase. Injector and FID detector temperatures were set at 483 K and 523 K, respectively. The column oven program included three steps, i.e. 3 min of constant temperature at 303 K, heating to 443 K at 10 K/min heating rate and cooling down to 443 K. This instrument provided a good separation of C4 hydrocarbons.

By combining results from these two GC analyses, it was possible to determine the ratio between different alkanes, -olefins and their isomers.

Chapter 3

Results and Discussion

3.1 *In-situ* DRIFT Spectroscopy

DRIFTS experiments were performed with different gas compositions in order to get more information about the specific influences of the different gasses on the reaction. H_2 and ethylene were always added in a 1:1 ratio during every experiment, but H_2 (10% of the total gas mixture) was varied. TEAl (10 μl) was not part of the gas composition, however it was also a variable and added to the catalyst before the reaction was started. The following different compositions were used:

- With H_2 and TEAl
- Only TEAl
- Only H_2
- Neither H_2 nor TEAl

TEAl reduces the induction time by helping to reduce the catalyst and scavenging of poisons while H_2 is reducing the molecular weight distribution by terminating the growing polymer chains more easily. [16] In all cases the gas phase was collected during the reaction for the GC(-MS) analysis.

Two different catalysts were analyzed (Table 2.1). The titanated catalyst CrTiSi-04, which contains 0.98 wt% Cr and 4.7 wt% Ti and the non-titanated catalyst CrSi-01, which contains $\pm$ 0.5 wt% Cr and no Ti. It has to be noted that both catalyst contain a different loading of Cr.

Figure 3.1(a) shows the results in the CHx stretching region during *in situ* polymerization of ehtylene with TEAl and H_2 (left) and with TEAl and without H_2 (right) for both CrTiSi-04(blue) and CrSi-01 (red) catalysts. In all four cases the spectra were taken every half a minute and polyethylene is formed within time, as shown by the increasing CHx stretching bands at around 2926, 2855 and 2681 cm^{-1}. In the first spectra, the CHx stretching bands of the added TEAl in heptane are still visible. With ongoing polymerization, CHx stretching bands are rising till saturation of the signal is reached. From these DRIFTS spectra no noticeable differences due to the added H_2 can be seen.

Figure 3.1(b) shows the results without added co-catalyst. The absence of TEAl leads to much lower intensities. Furthermore, the bands show a blue shift, around 2940 and 2870 cm^{-1} due to decreased interactions between forming polymer chains, *i.e.* the chains are more isolated. The titanated catalyst, CrTiSi-04, shows slightly better reactivity in the reaction without TEAl than the non-titanated one.

In Figure 3.2, the ν(OH) regions for both catalysts are shown. For the titanated catalyst (Figure 3.2(a) spectra 1-2) two bands are seen at 3746 and 3695 cm^{-1} and also a shoulder at 3720 cm^{-1}, which is due to Ti interacting with OH groups. The band at 3746 cm^{-1} arises from isolated silanol groups and shifts towards 3695 cm^{-1} during the reaction with ethylene, due to the interaction with forming alkyl chains of the growing polymer, which was also noted by Barzan *et al.*, [17] Groppo *et al.* [26, 27] and Bordiga *et al.*[28] Those two bands shift around an isosbestic point at 3707 cm^{-1}. This means

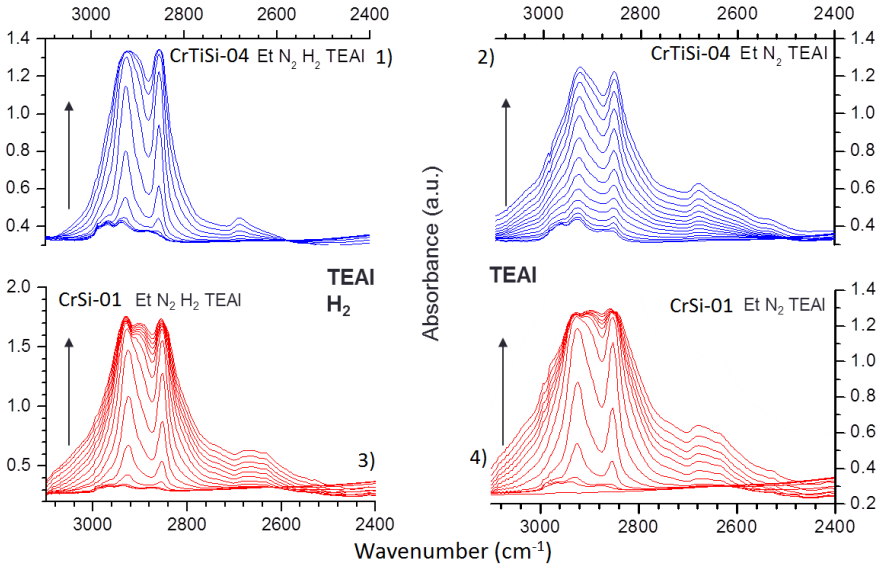

(a)

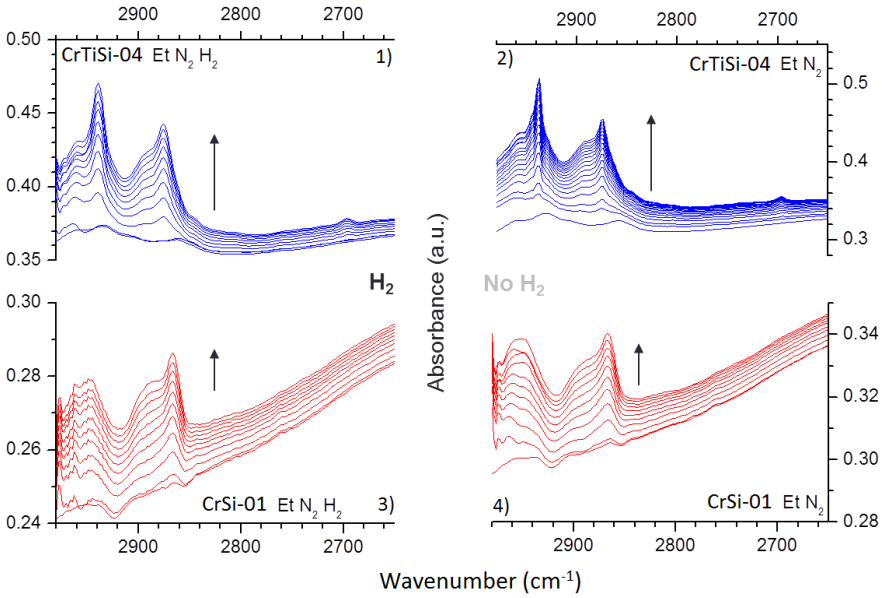

(b)

Figure 3.1: The CHx stretching region of CrTiSi-04 (blue) and CrSi-01 (red) Phillips $Cr/TiO_2/SiO_2$ catalysts. (a) Represents the gas composition with the TEAl co-catalyst and with or without H_2. (b) Represents the gas composition without TEAl co-catalyst and with or without H_2. Arrows indicate evolution in time.

that one specie is converted into another at the same time.[1]

The ν(OH) region of the non-titanated catalyst does not show an obvious isosbestic point, probably because of the movement of the sample with growing polymer. However, the bands at 3746 and 3695 cm^{-1} show the same behavior as for the titanated catalyst. The band belonging to the isolated silanols groups shifts to lower wavenumbers due to the interaction with forming alkyl chains. Furthermore, an

[1] *i.e.* an isosbestic point indicates that the stoichiometry of the reaction remains unchanged during the chemical reaction or the physical change of the catalyst. Also, no secondary reactions occurring during the considered time range. [29]

extra band is appearing at 3605 cm^{-1} in the ν(OH) spectra of CrSi-01 and probably comes from the interaction of the SiOH group with an adjacent Lewis acidic chromium center, Si-(μ-OH)-Cr. [30, 31]. According to Jozwiak *et.al.* the shift from 3746 to 3695 cm^{-1} appears to relate to the temperature of catalyst dehydroxylation rather than to the degree of polymerization. The 3605 cm^{-1} band should indicate an advanced polymerization stage, which is always present in commercial PE films. [31]

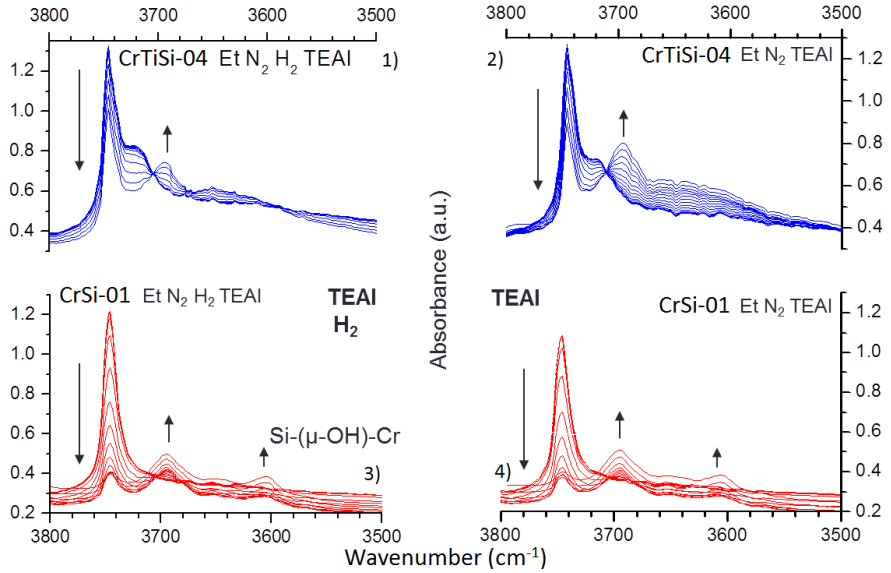

(a)

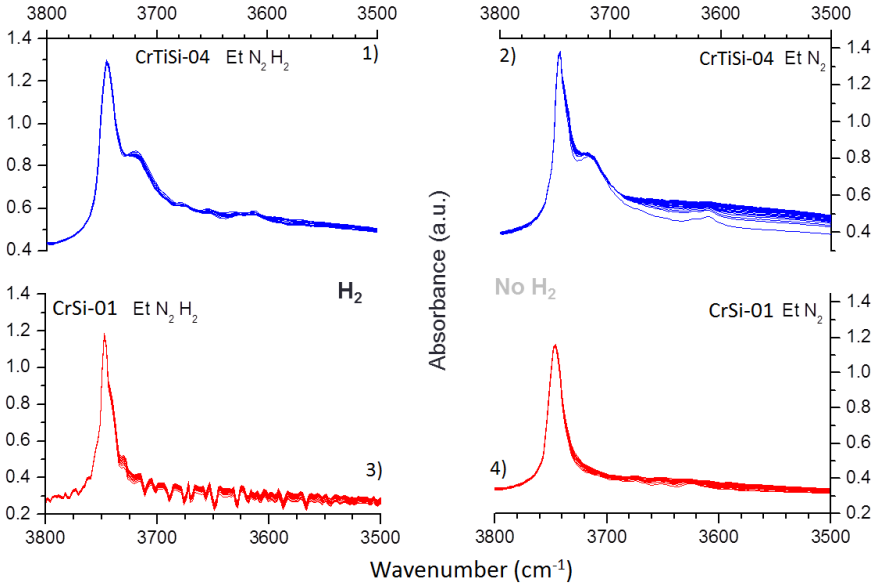

(b)

Figure 3.2: The OH region of CrTiSi-04 (blue) and CrSi-01 (red). (a) Represents the gas composition with the TEAl co-catalyst and with or without H_2. (b) Represents the gas composition without TEAl co-catalyst and with or without H_2. Arrows indicate evolution in time.

The OH stretching region, in the experiments without TEAl, is illustrated in Figure 3.2(b). For both the titanated and non-titanated catalyst no shifts or interactions can be distinguished, simply due the fact that the intensity changes are too low to detect any shift.

3.2 *In-situ* UV-Vis-NIR Diffuse Reflectance Spectroscopy

With the *in-situ* UV-VIS-NIR DRS measurements one can investigate the forming of polymer (NIR region), as well as follow the electronic changes of the catalyst (UV-Vis region). By simultaneously inspecting the UV-VIS and the NIR region it is possible to monitor the reduction of activated Cr^{6+} to Cr in lower oxidation states which are considered as active species, [2**?**] influence of Ti and detect forming PE in order to elucidate the mechanism of polymerization. Besides the combination bands of the forming polymer, the first and second overtones of these vibrations can also be detected according to Watari (Table 3.1). [32]

Table 3.1: Assignment of the CHx overtone and combination bands in the NIR spectra. [32]

Assignment	Wavenumber (cm^{-1})
CH str second overtone (CH_2)	8569
CH str second overtone (CH_3)	8428
CH str second overtone (CH_2)	8218
2CH str + CH def (CH_2)	7177
2CH str + CH def (CH_2)	7064
2CH str + CH def (CH_2)	6952
Combination (CH_2)	6486
Combination (CH_3)	6112
Combination (CH_2)	5846
CH str first overtone (CH_2)	5777
CH str first overtone (CH_2)	5668

Reference measurements were performed. The first and second overtones of the CHx vibrations of LLDPE and HDPE provided by Total and the polyethylene after reaction in the DRIFTS cell using the CrSi-01 catalyst were measured and are illustrated in Figures 3.3 and 3.4. This showed the possibility of detection of the *in-situ* produced PE.

The advantages of using the Cary 500 instrument over UV-VIS probe is not only that it is possible to obtain spectra of much better quality and S/N ratio, it also enables to actually measure the spectrum of $O \rightarrow Cr^{6+}$ charge transfer (CT) bands in the UV region, which is not possible with the probe.

For the *in-situ* UV-Vis-NIR DRS measurements the same mass flow controller setup was used as for DRIFTS, but with another quartz reactor. For these experiments catalysts were used which contained the same amount of chromium (0.5 wt% Cr) but a different loading of Ti (0-4.7 wt% Ti), for comparison. From DRIFTS experiments it was clear that in the absence of the TEAl co-catalyst, the signal was too low. Therefore the UV-Vis-NIR DRS experiments were performed with only TEAl as the co-catalyst. The gas phase was collected during the reaction for the GC(-MS) analysis. GC-MS was performed on some samples in order to identify the different products formed, while GC was performed on all of the sampled gas mixtures as well, in order to detect lower olefins, *i.e.* butenes, and to quantitatively analyze the composition of the gas phase. This was not possible with the combination of GC-MS because of the short retention time of butenes.

Figure 3.6 shows the results for the non titanated catalyst, CrSi-01, with H_2 (a) and without H_2 (b). The main spectra shows the UV-Vis region, where the electronic changes of the catalyst can be seen. The inset in the graph shows the combination bands of the polymer in the NIR region while forming within time. The three bands in spectral ranges of 37600-39600, 27000-31000 and ≈21000 cm^{-1} belong to the Cr^{6+} specie of the active catalyst. These are $O \rightarrow Cr^{6+}$ charge transfer bands and decrease during the reaction, because these sites are being reduced and converted into $Cr^{3+/2+}$

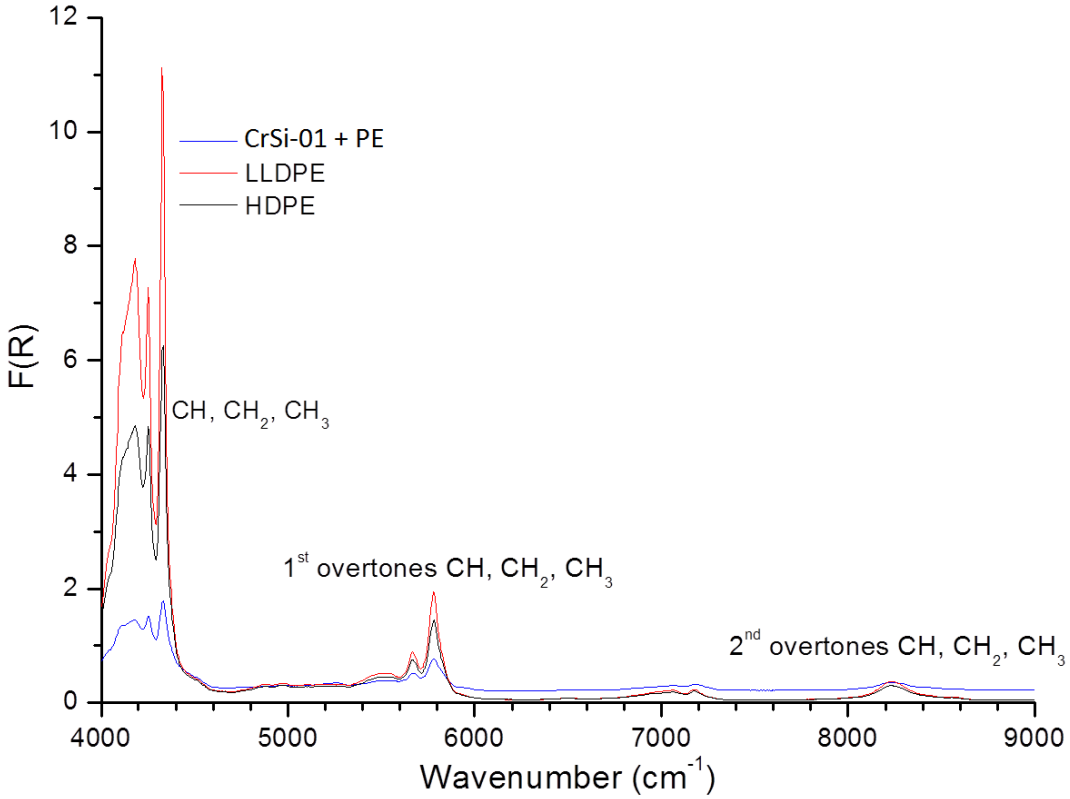

Figure 3.3: NIR region with the first and second overtones of the CHx vibrations of LLDPE, HDPE and CrSi-01PE.

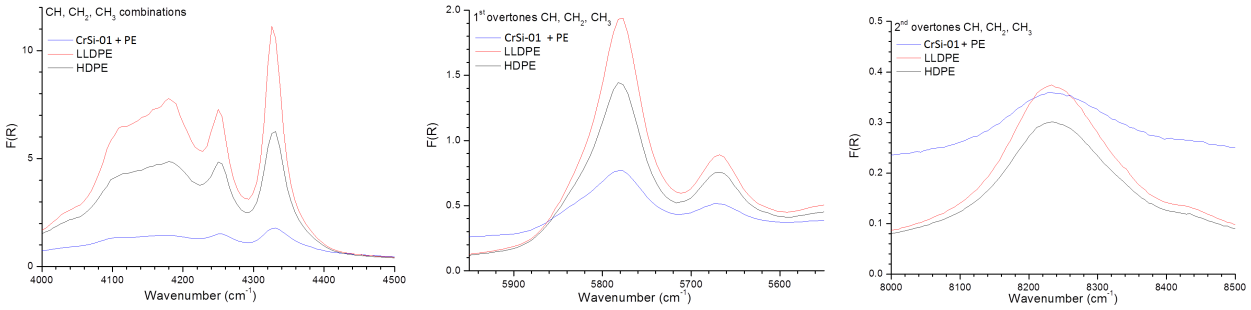

(a) (b) (c)

Figure 3.4: Combination bands (a) and first (b) and second (c) overtones of LLDPE and HDPE provided by Total and polyethylene catalyzed over CrSi-01.

Table 3.2: Overview of catalysts used for UV-Vis-NIR DRS experiments.

Catalyst	Act. Temp. (K)	Cr^{n+}	wt% Cr	wt% Ti
CrSi-01	1048	Cr^{6+}	0.5	0
CrTiSi-02	1048	Cr^{6+}	0.5	2.2
CrTiSi-03	1048	Cr^{6+}	0.5	4
CrTiSi-04	1048	Cr^{6+}	0.98	4.7

species. The band rising at ≈16000 cm^{-1} can be assigned to a d-d transition of the forming $Cr^{3+/2+}$ species. [33] The bands are shifting around an isosbestic point at ≈18500 cm^{-1} (highlighted by a ∘ in

the graphs), which means that one species is converted into another species at the same time. This is consistent with the 1 to 1 conversion of Cr^{6+} species into $Cr^{3+/2+}$ species. An overview of all the electronic and vibrational assignments of the bands is given in Table 3.3.

Table 3.3: Assignment of the electronic and vibrational bands in the UV-Vis-NIR DRS. CT = Charge Transfer.

	Assignment	$\widetilde{\nu}(cm^{-1})$
Electronic	$O \rightarrow Cr^{6+}$ CT	37600-39600
	$O \rightarrow Cr^{6+}$ CT	27000-31000
	$O \rightarrow Cr^{6+}$ CT	21000
	Cr^{3+} d-d	16000
Vibrational	$3\nu_{as}(CH_2)$	8423, 8233
	$2\nu(SiOH)$	7325
	$2\nu_{as/s}(CH_2) + \delta(CH_2)$	7189, 7059
		6966, 6482
	$2\nu_{as/s}(CH_2)$	5777, 5668
	$\nu(H_2O) + \delta(H_2O)$	5260
	$\nu(SiOH) + \delta(SiOH)$	4525
	$\nu_{as/s}(CH_2) + \delta(CH_2)$	4325,4250
	$\nu_{as}(CH_2) + w(CH_2)$	4185

The same shifts can be observed for the CrTiSi-02 catalyst, which contains 2.2 wt% Ti, catalyst CrTiSi-03, which contains 4 wt% Ti and catalyst CrTiSi-04, which contains 4.7 wt% Ti, as shown in Figures 3.7, 3.8 and 3.9 respectively. From these results, it was observed that in general the catalyst is more reduced when H_2 is present in the gas mixture, *i.e* more Cr^{6+} species are converted into $Cr^{3+/2+}$ species. This does not automatically mean that the catalyst is more active if H_2 is present, since H_2 does not necessarily reduces only the active polymerization sites of the catalyst. Because of the low amount of these sites, mostly the inactive polymerization sites of the catalyst are being reduced.

A trend that is observed for these three catalysts with increasing Ti loading, is that the three bands belonging to $O \rightarrow Cr^{6+}$ CT shift towards lower wavenumbers when the amount of Ti is increased. Probably due to the smaller electron cloud that comes with Ti, which causes a smaller band gap for the $O \rightarrow Cr^{6+}$ charge transfer. A schematic representation of this is illustrated in Figure 3.5. As can be seen from the electronegativity chart, Ti is less electronegative than Si. When Si is replaced by Ti, the electron pair that belongs to that bond is more drawn to the oxygen and thereby more electrons are closer to the Cr site. This makes the band gap between O and Cr smaller, decreases the energy needed for transition, which causes the shift towards lower wavenumbers when more Ti is added to the catalyst. No formed olefins can be detected with UV-Vis-NIR DRS. Therefore, the gas was collected for GC(-MS)analysis and will be discussed in Section 3.4.2.

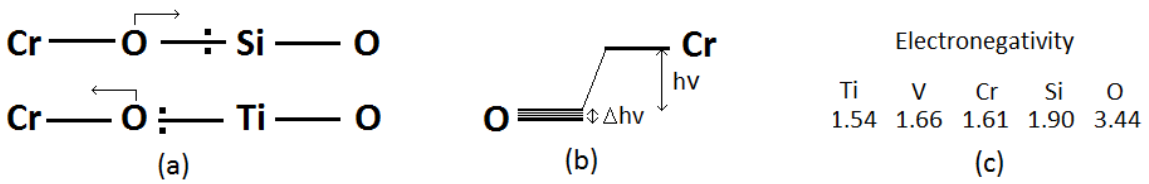

Figure 3.5: Schematic drawing of the electronic effect of Ti. (a) Illustrates where the electrons density is higher, (b) shows a drop for the band gap between O and Cr and (c) gives an indication of the electronegativity of the different elements present.

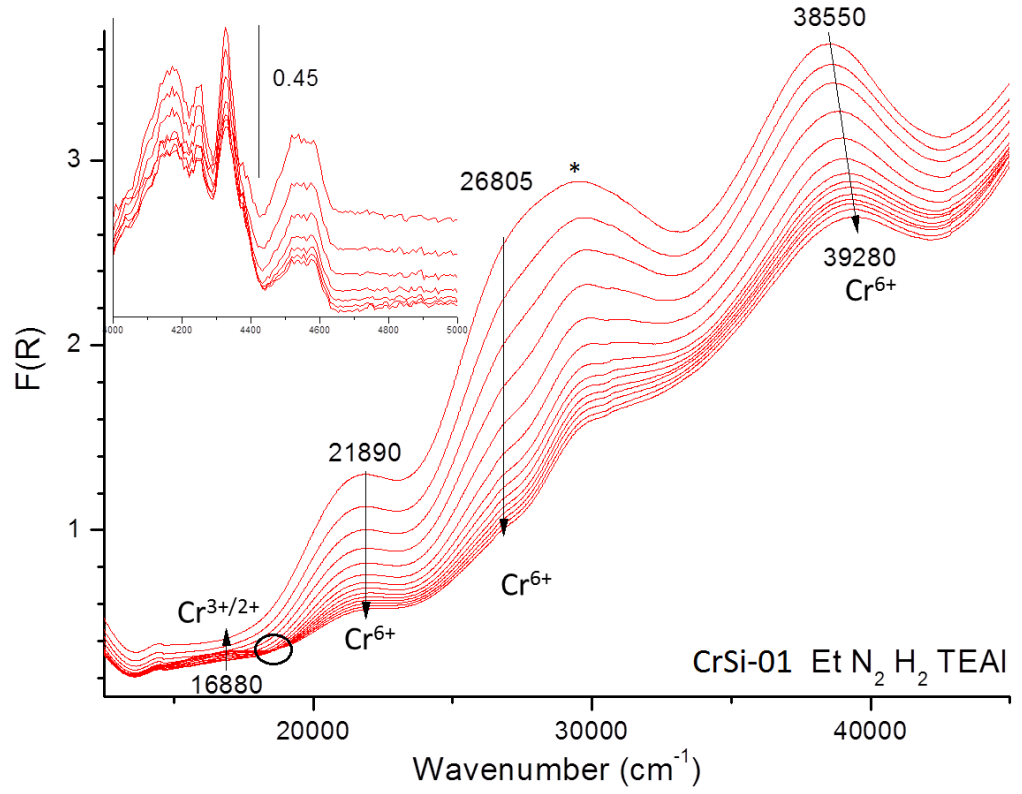

(a)

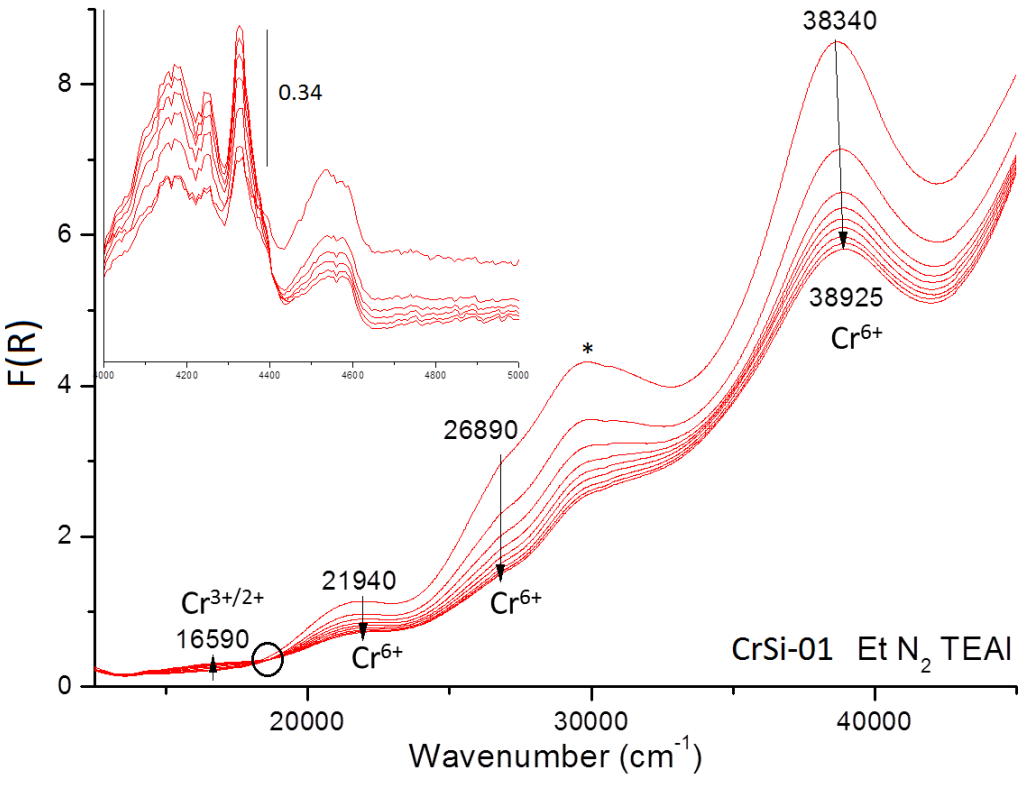

(b)

Figure 3.6: UV-Vis area of catalyst CrSi-01 with H_2 (a) and without H_2 (b). The electronic changes are illustrated in the main spectra, the inset shows the NIR area of the forming polyethylene. The isosbestic point is marked by the ∘. The band indicated by the * between 29000 and 30000 cm^{-1} is caused by when the jump, in changing source of the apparatus, is smoothed.

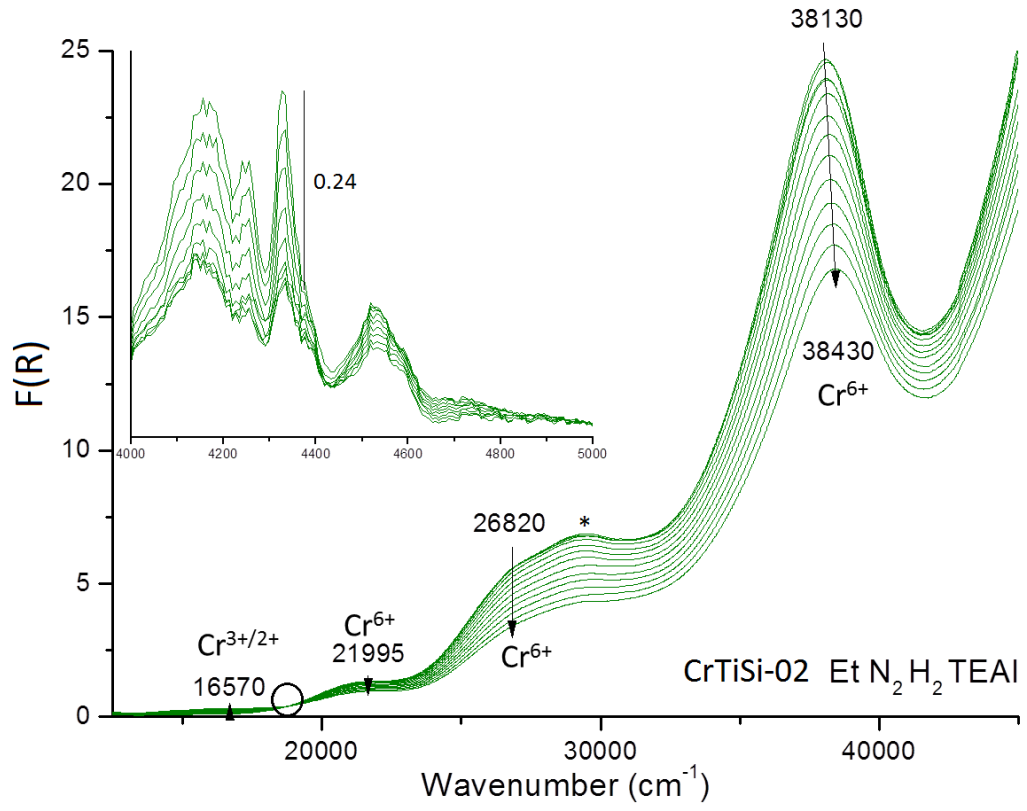

(a)

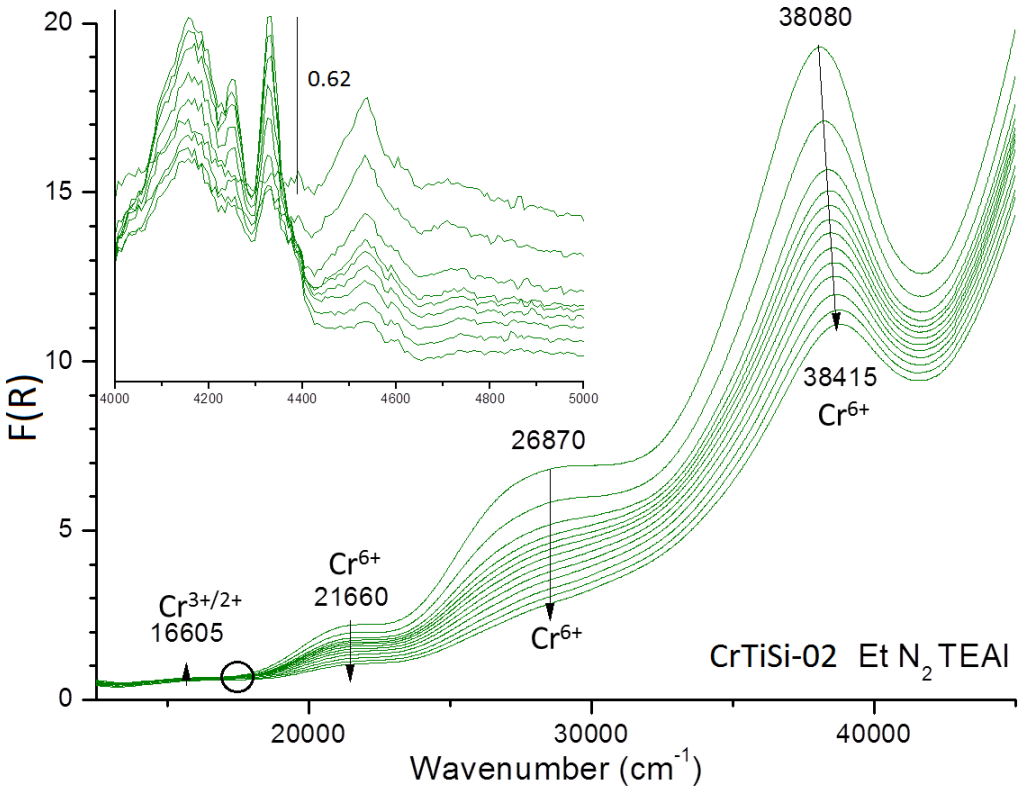

(b)

Figure 3.7: UV-Vis area of catalyst CrTiSi-02 with H_2 (a) and without H_2 (b). The electronic changes are illustrated in the main spectra, the inset shows the NIR area of the forming polyethylene. The isosbestic point is marked by the ∘. The band indicated by the * between 29000 and 30000 cm^{-1} is caused by when the jump, in changing source of the apparatus, is smoothed.

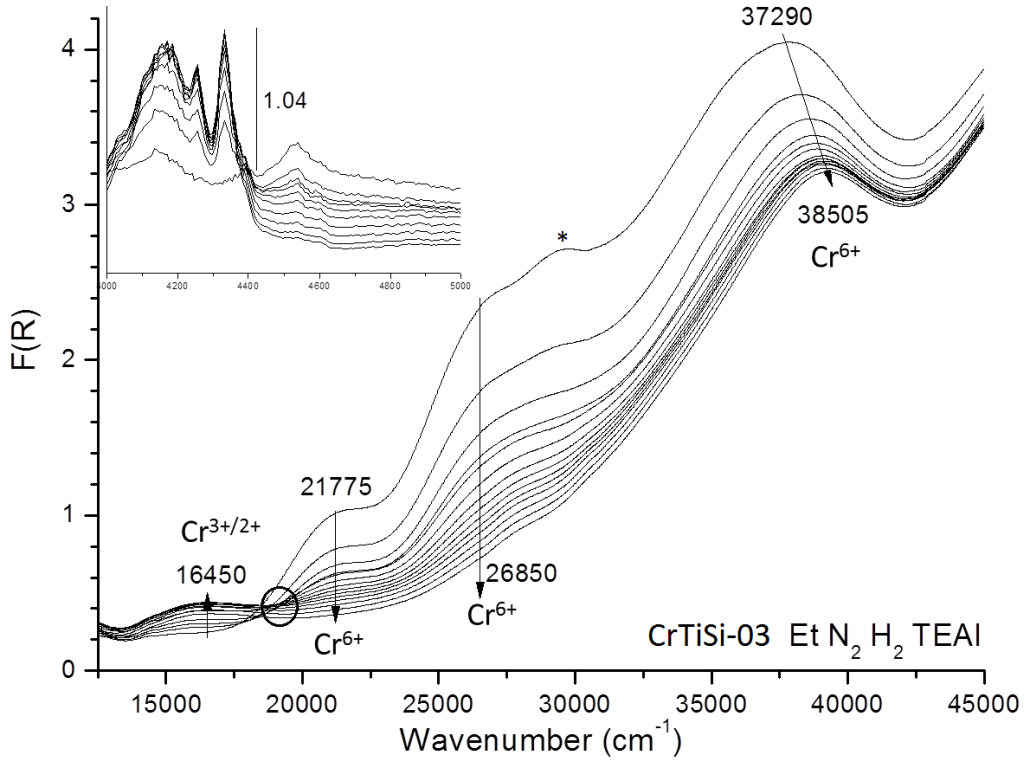

(a)

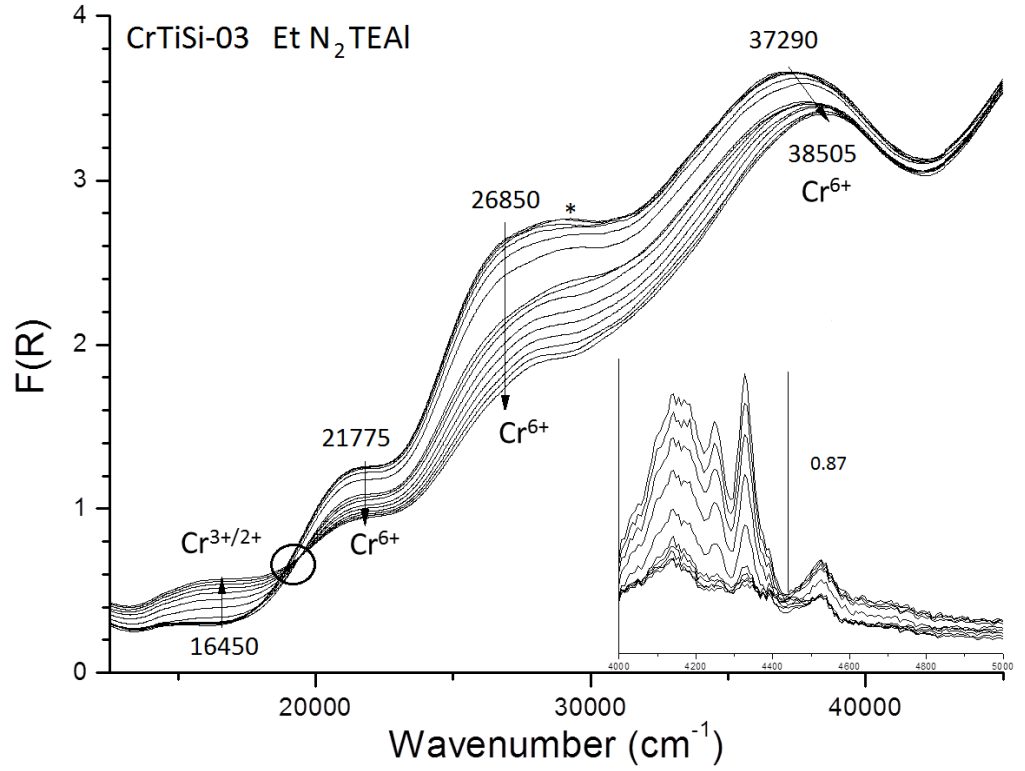

(b)

Figure 3.8: UV-Vis area of catalyst CrTiSi-03 with H_2 (a) and without H_2 (b). The electronic changes are illustrated in the main spectra, the inset shows the NIR area of the forming polyethylene. The isosbestic point is marked by the ∘. The band indicated by the * between 29000 and 30000 cm^{-1} is caused by when the jump, in changing source of the apparatus, is smoothed.

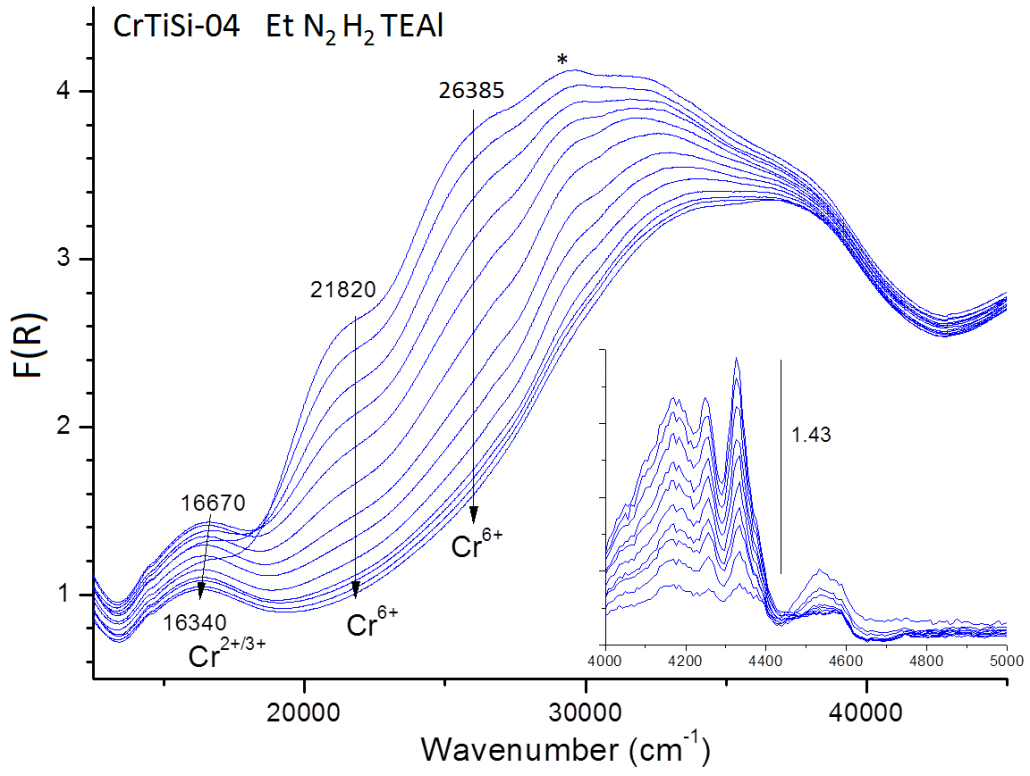

(a)

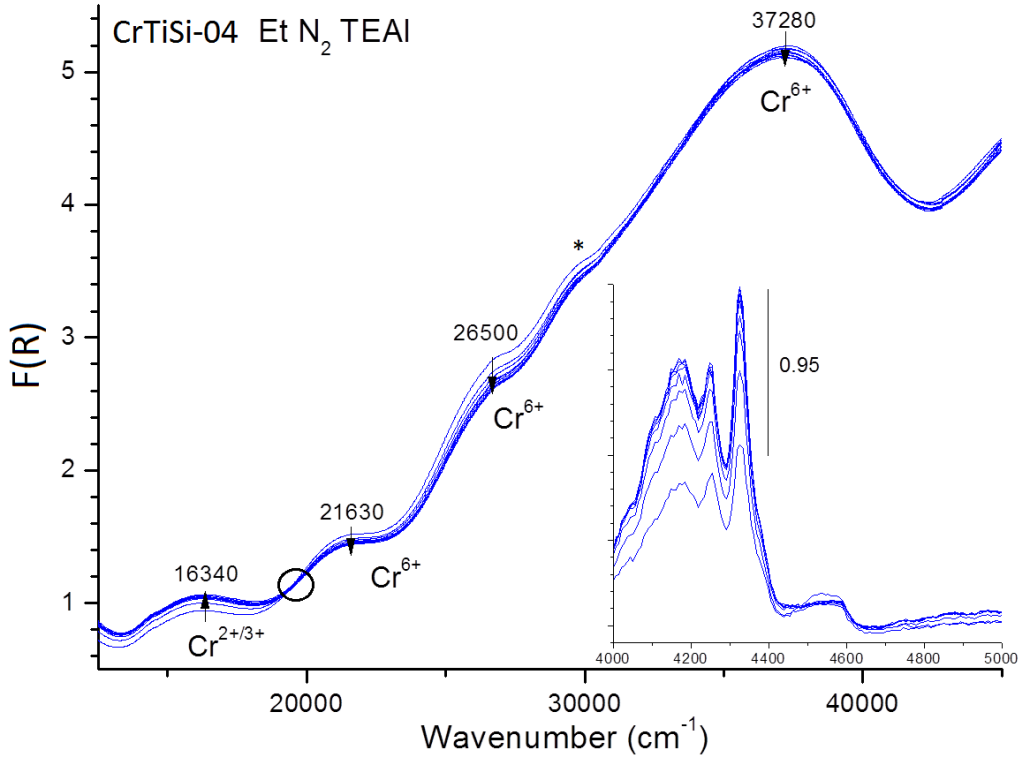

(b)

Figure 3.9: UV-Vis area of catalyst CrTiSi-04 with H_2 (a) and without H_2 (b). The electronic changes are illustrated in the main spectra, the inset shows the NIR area of the forming polyethylene. The isosbestic point is marked by the ∘. The band indicated by the * between 29000 and 30000 cm^{-1} is caused by when the jump, in changing source of the apparatus, is smoothed.

3.3 Transmission FT-IR Spectroscopy

Because there could be no olefins detected with DRIFTS, due to the overlap with the vibrations of ethylene, FT-IR experiments were performed as well in order to detect possible crystallinity within the formed polymer and indirectly try to see if oligomers were formed. The broad band at 1100 cm^{-1} in Figure 3.10 belongs to the silica support of the catalyst. However, the bands at 2920 and 2851 cm^{-1} belong to the ν(CHx) of the polyethylene. At lower wavenumbers at 729 and 718 cm^{-1} (CH_2 rocking vibrations) two bands can be noted, which give information about the crystallinity of the polymer. For highly crystalline structures, these two bands are expected to be of equal height. From the inset of Figure 3.10 it is clear that the the bands are not of equal height and the polymer is not highly crystalline. This might be an indication of branching in the polymer chains by *in-situ* formed olefins. Because the branching is random, it prevents the forming polymer chain to be able to arrange itself in a crystal-like structure.

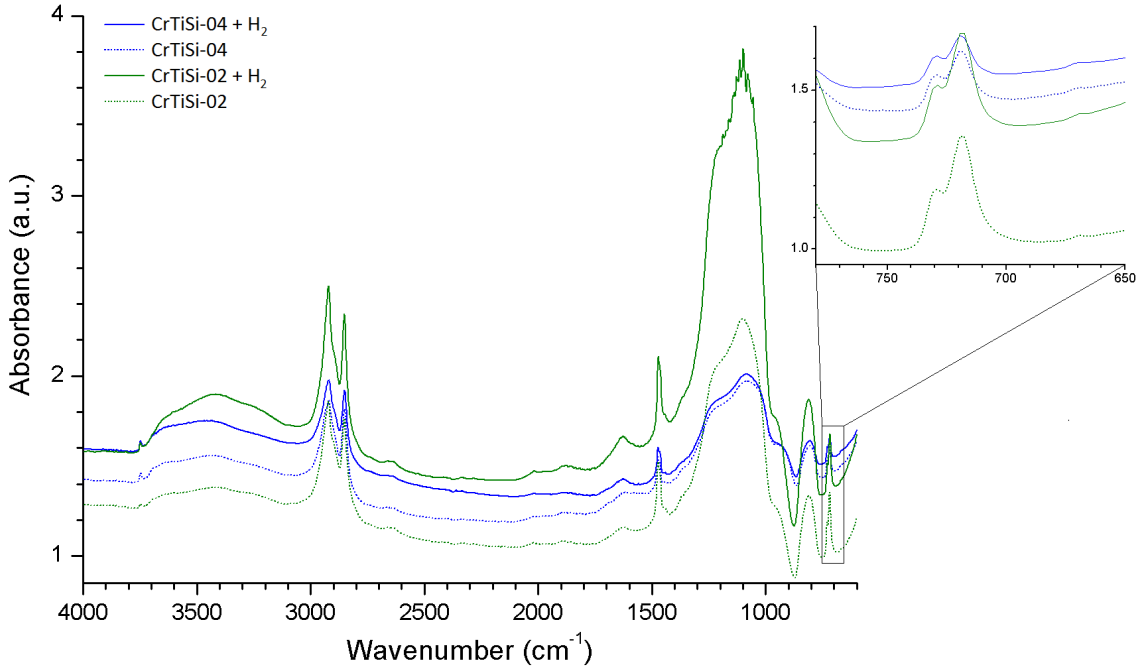

Figure 3.10: Transmission FT-IR spectra of the CrTiSi-02 and CrTiSi-04 catalysts. Inset shows the crystallinity of the polyethylene.

3.4 GC-MS

In order to investigate if there were indeed olefins formed, GC-MS analysis was performed of the gas phase collected during the DRIFTS and UV-Vis-NIR experiments. With the combination of Gas Chromatography and Mass Spectrometry it is possible to separate different components within the gas mixture, identify and compare those components with a library of known mass spectra.

3.4.1 GC-MS from the DRIFTS Experiments

Figure 3.11 shows the non-titanated CrSi-01 catalyst with all of the possible combination of gas mixtures. Also, a blank experiment was performed with KBr instead of the catalyst with a gas reactant mixture, containing ethylene, H_2 and the TEAl co-catalyst. The peaks appearing within the blank experiment are due to the heptanes used as TEAl solvents. Reactions run without TEAl show no additional bands. The heptane bands in the spectra with the mixture of ethylene and H_2 are probably due to contamination of the syringe used for injections. The reactions which contain TEAl

in the mixture show some extra bands before the heptanes come off. This is the region of interest and more detailed spectra are shown in Figures 3.12 and 3.13. Different hexenes are formed, however with the main fraction being 1-hexene. In the reaction which contains both TEAl and H_2 it is seen that more hexanes are being formed, most probably due to the hydrogenation of some hexenes. A cyclic product is also being formed, which could be an indication that there is a different mechanism for olefin forming than for the polymerization.

C4 fractions could not be detected because with the current column and analysis conditions, the retention times of these fractions were too short to detect with the MS detector, due to the overlap with a dominant ethylene peak. On the other hand, if only GC was performed, the C4 fractions could be detected. This is shown in Section 3.4.2.

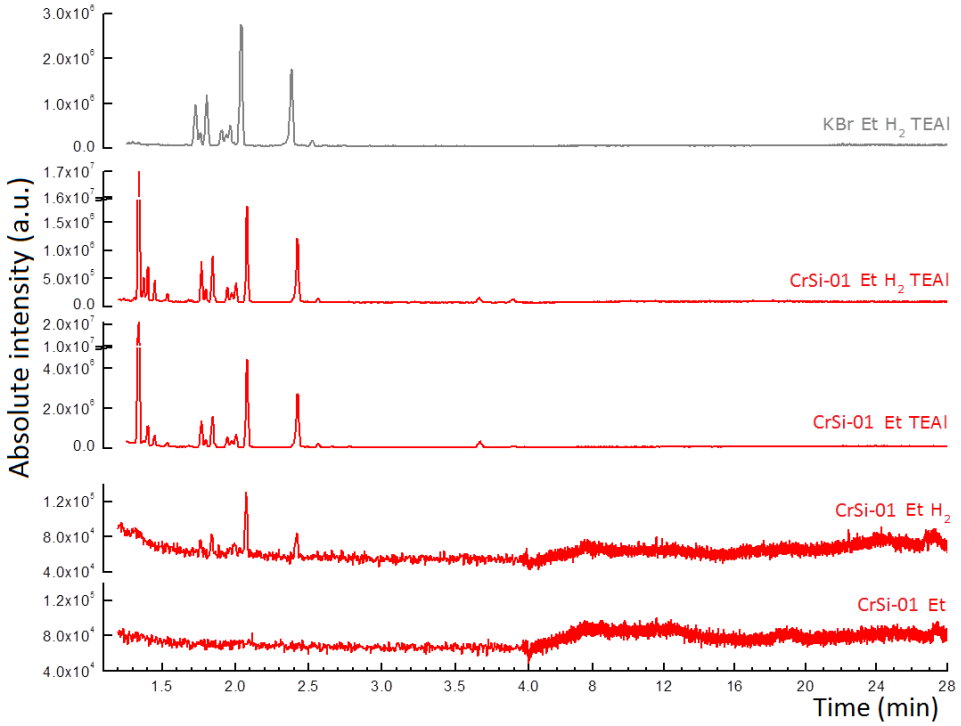

Figure 3.11: GC-MS chromatograph of the non-titanated catalyst CrSi-01, with all the different gas mixtures.

The same analysis was performed for the gas mixtures from the polymerization with the titanated catalyst, CrTiSi-04. The same can be observed as for the non-titanated catalyst, *i.e*, the same products are being formed with the main fraction being 1-hexene. In the mixture which contains TEAl and H_2, more of the hexenes were getting hydrogenated into hexanes. However, none or no significant amount of cyclic product is formed with the titanated catalyst.

Table 3.4 shows the integrated peaks versus heptane peak area in order to provide information about the quantitative analysis. However, this method is just an estimation given that GC-MS cannot be used as a method for accurate quantitative analysis. For the non-titanated catalyst, polymerization with H_2 leads to more of the 1-hexene forming, as well as hydrogenation of hexenes and octenes. The same can be seen for the titanated catalyst. If both catalyst are compared with each other, it is clear that more 1-hexene is produced with the non-titanated catalyst. However, with the titanated one, more higher olefins (*i.e.*, C8 and C10) are produced compared to hexenes.

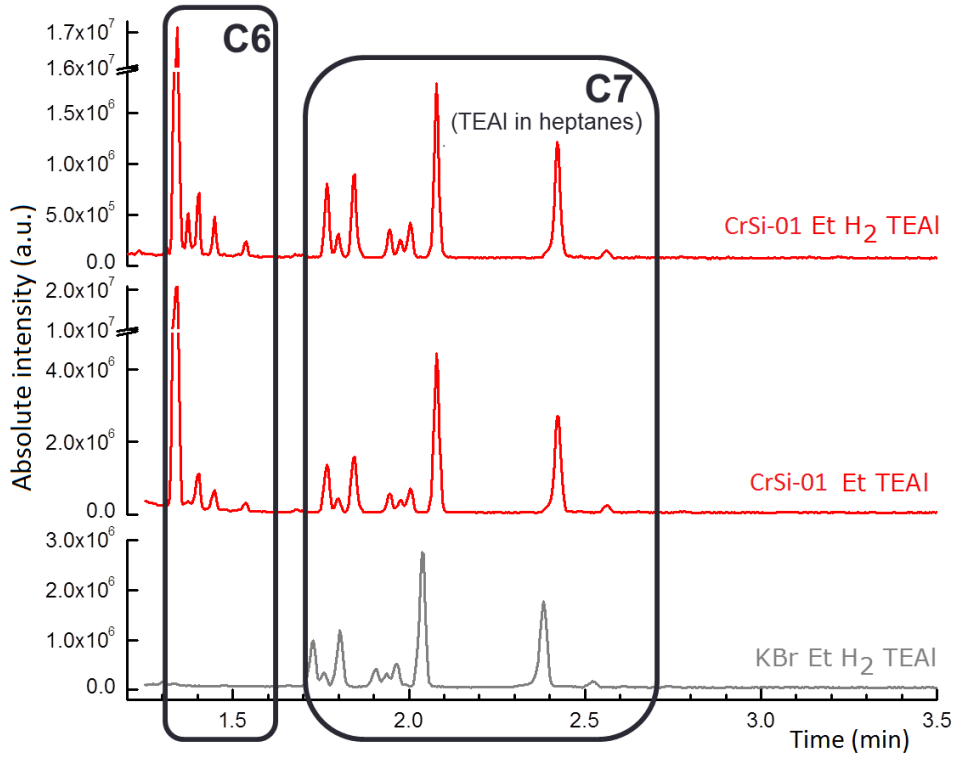

Figure 3.12: GC-MS chromatograph of the hexenes and heptanes for the non-titanated catalyst CrSi-01, with co-catalyst TEAl.

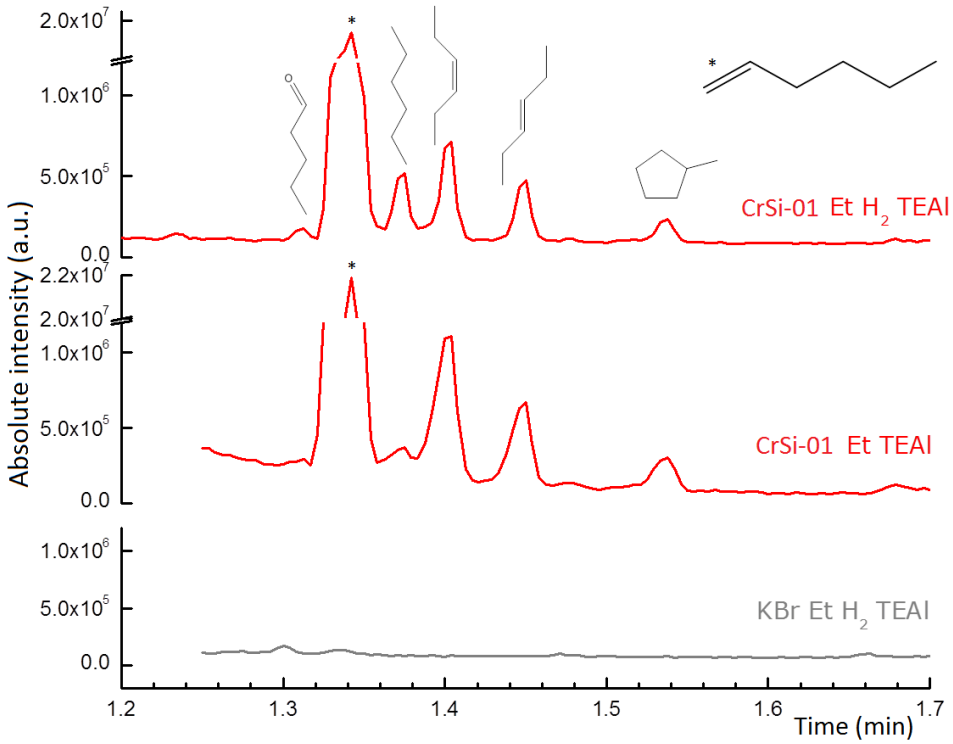

Figure 3.13: GC-MS chromatograph of non-titanated catalyst CrSi-01, with the assigned hexene peaks.

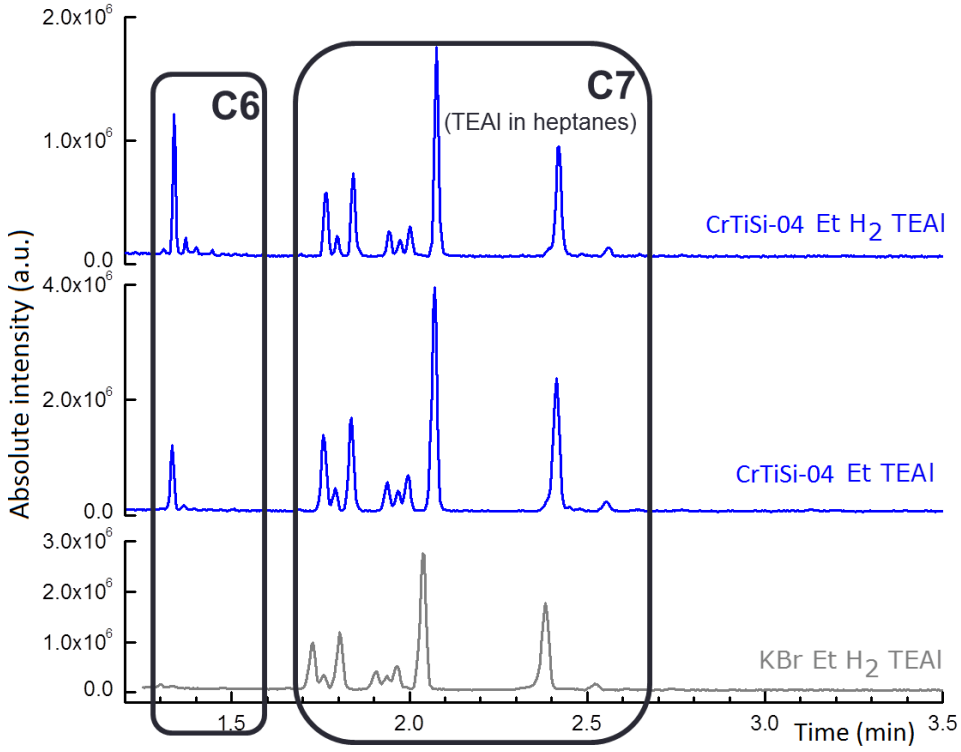

Figure 3.14: GC-MS chromatograph of the hexenes and heptanes for the titanated catalyst CrTiSi-04, with co-catalyst TEAl.

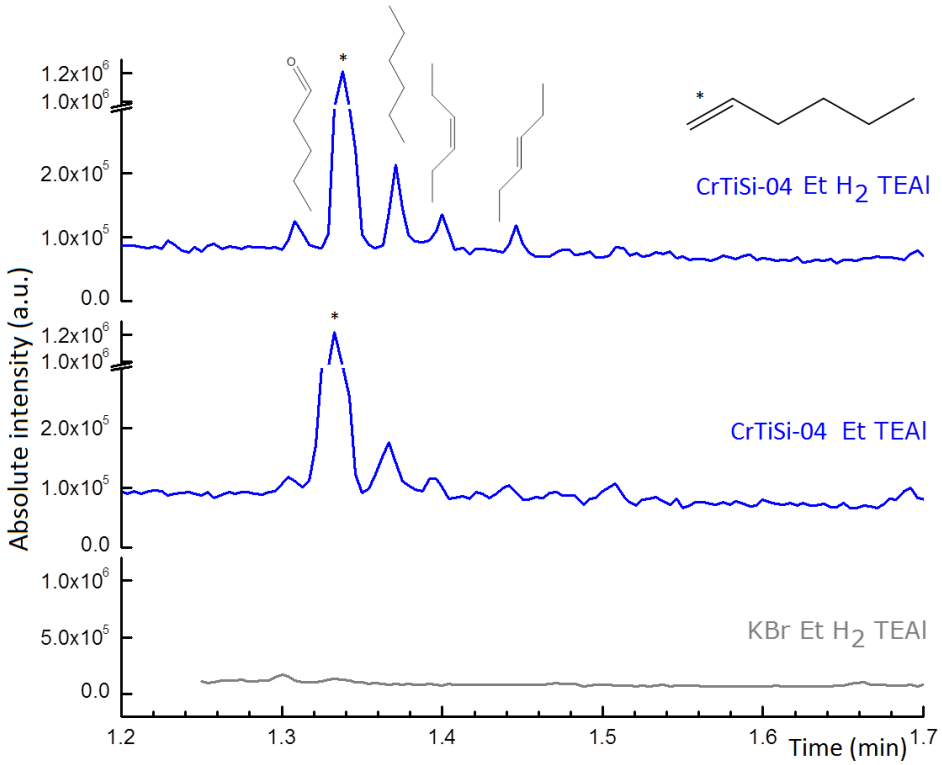

Figure 3.15: GC-MS chromatograph of titanated catalyst CrTiSi-04, with the assigned hexene peaks.

Table 3.4: Integrated peak areas of oligomerization product versus the reference heptane peak area used as internal standard.

Catalyst	CrSi-01		CrTiSi-04	
Component	H_2	No H_2	H_2	No H_2
Pentanal	0.023	0.004	0.015	0.003
1-Hexene	6.298	3.969	0.432	0.192
Hexane	0.117	0.008	0.040	0.015
Cis-3-hexene	0.226	0.164	0.015	0.004
Trans-3-hexene	0.148	0.097	0.012	0.000
Methylcyclopentane	0.061	0.042	0.000	0.004
Methylcyclopentene	0.015	0.022	0.000	0.007
Heptane	1.000	1.000	1.000	1.000
1-Octene	0.086	0.119	0.165	0.100
Octane	0.070	0.022	0.036	0.013
3-Octene	0.000	0.018	0.000	0.000
3-Octene	0.000	0.013	0.000	0.000
Decene	0.000	0.016	0.000	0.000
Dodecene	0.051	0.015	0.000	0.000
Dodecene	0.000	0.017	0.033	0.026
Dodecene	0.042	0.017	0.032	0.011

3.4.2 GC-MS from the UV-Vis-NIR DRS Experiments

Similar as with the gas phase collected during the DRIFTS measurement, GC-MS was performed on some of the sampled gas of the UV-Vis-NIR DRS experiments to determine if the same products were formed as during the DRIFTS experiments. Butenes could not be detected with the current column and analysis conditions on the GC-MS. In order to detect these species formed and quantify results, only GC was performed on all the sampled gas from the UV-Vis-NIR DRS experiments.

For these experiments also the CrTiSi-04 catalyst that contained 4.7 wt% Ti and 1 wt% Cr was included in the results.

Hydrocarbon distribution and productivity

Figure 3.16(a) shows the results for the hydrocarbon productivity in ethylene polymerization reactions with and without H_2 for four different catalysts, including experiments performed with only silica support and titanated silica support. In general, the amount of produced hydrocarbons decreases with increasing Ti loading. Furthermore, it is observed that with the increasing of Ti loading the ratio between C6 and C4 oligomers decreases. This is more clear on Figure 3.16(b), where the hydrocarbon distribution is presented by setting the total amount of the produced hydrocarbons to 100%. Moreover, all the different observed hydrocarbons, are included, *i.e.* different olefins and paraffins.

The amount of produced 1-hexene is decreased with increasing Ti loading, as is seen if we compare the CrSi-01, CrTiSi-02 and CrTiSi-03 catalysts (Figure 3.16(b)). Furthermore, in the cases where no H_2 was present in the gas phase, there was more 1-hexene formed. Which we have also confirmed in the GC-MS measurements of the sampled gas from the DRIFTS experiments.

Figure 3.16(b) can be split into a paraffins and an olefins part (Figures 3.17 and 3.18, respectively). From the paraffin distribution it can be concluded that with increasing Ti loading the selectivity towards paraffins formed increases. When H_2 is added into the gas mixture, the selectivity towards hydrocarbons increases. Figure 3.17(b) shows that the selectivity towards butanes increases when no H_2 is added. From the olefin distribution (Figure 3.18(b)) it can be concluded that when the Ti loading increases the selectivity towards butenes increases and towards hexenes decreases. Moreover, the overall amount of olefins decreases with increasing Ti loading.

In general, the addition of H_2 increases the hydrocarbon yield. Furthermore, H_2 decreases the selectivity towards unsaturated hydrocarbons (olefins) and increases selectivity towards saturated hydrocarbons (paraffins). Addition of H_2 promotes selectivity to hexane and octane at the expense of butane selectivity, changing the distribution of paraffin products. However, H_2 does not substantially change the ratios of olefins (butenes, hexenes and octenes).

Furthermore, the influence of Ti seems of great importance as well. Increase of Ti loading decreases overall hydrocarbon productivity. It also causes a lowering in the selectivity towards olefins while it increases the selectivity towards paraffins. The distribution of parraffins is not influenced by changes in Ti loading. However, it does influence the olefin distribution, increase of Ti decreases the selectivity towards hexenes and increases selectivity towards butenes.

Anderson-Schultz-Flory distribution

These data can be plotted according the Anderson-Schultz-Flory (ASF) linear insertion distribution. [34] The ASF distribution is a mathematical function that describes the relative ratios of polymers of different length after polymerization, which is based on their relative probabilities of occurrence in the mixture and implies that shorter polymers are favored over longer polymer chains. If the $\log(W_n/n)$, where W_n is the mass fraction of the species with carbon number n from the GC data, is plotted against the number of carbons in the chain, it should give a straight line if the oligomers are following the ASF distribution. Figures 3.19 and 3.20 illustrate the ASF distribution for the varying amount of

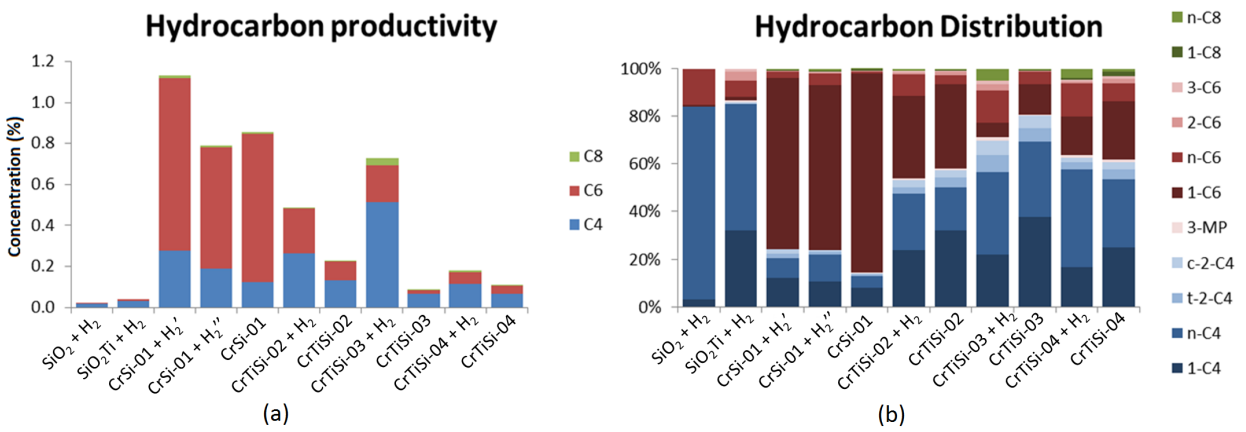

Figure 3.16: Hydrocarbon productivity and distribution of the C4, C6 and C8 sections of the gas phase from UV-Vis-NIR DRS.

Ff

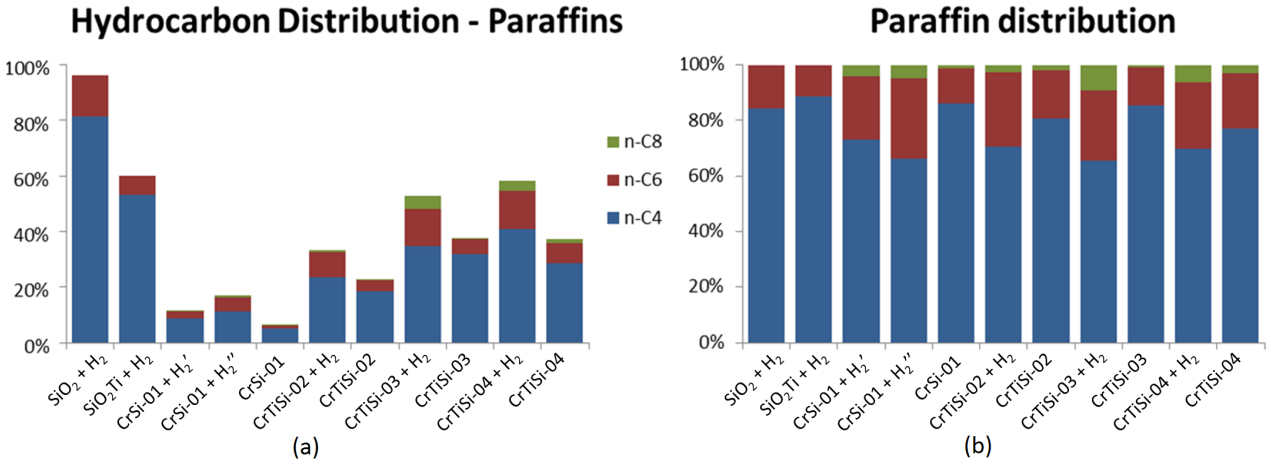

Figure 3.17: (a) Hydrocarbon distributions of the main paraffins, when Figure 3.16(a) is separated into paraffins and olefins distribution. (b) The amount of the different paraffins within the paraffin distribution.

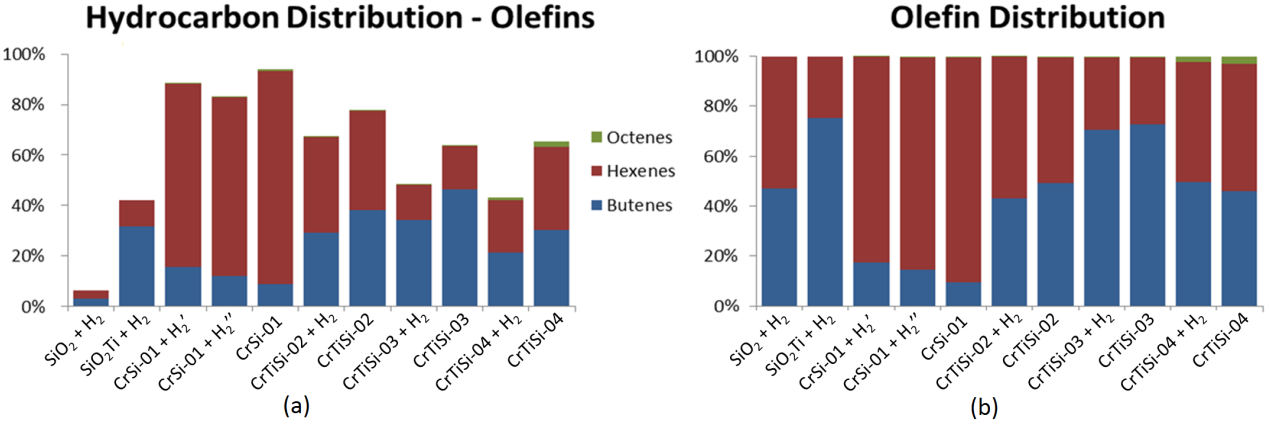

Figure 3.18: (a) Hydrocarbon distribution of the main olefins, when Figure 3.16(a) is separated into paraffins and olefins distribution. (b) The amount of different olefins within the olefin distribution.

Ti and the amount of Cr, respectively, present in the different Phillips catalysts.

In Figure 3.19 the catalysts are shown which differ in the amount of Ti from 0-4 wt% Ti. The darker blue the line is, the more Ti the catalyst contains. From the olefin distribution (Figure 3.19(a)) it can be seen that with increasing amount of Ti the curve becomes more linear due to the decreasing selectivity towards hexenes. This might be an indication that there is another mechanism valid for the formation of hexenes (or olefins in general) other then linear insertion, which causes the break of the linearity in the ASF distribution. For the paraffin distribution there is more or less a straight line visible.

The same analysis is performed with varying the amount of Cr (Figure 3.20). A slight selectivity towards hexenes within the olefins, when more Cr is present in the catalyst, can be noted. Among the paraffins, the amount of Cr makes no difference as it is following the ASF distribution. It should be noted that there are only three points available for these calculations and that is might be the case that one of the other points is off line. However, in combination with all the other results (Figure 3.18(b)) it is more likely that there is a selectivity towards hexenes, which is caused by a different mechanism.

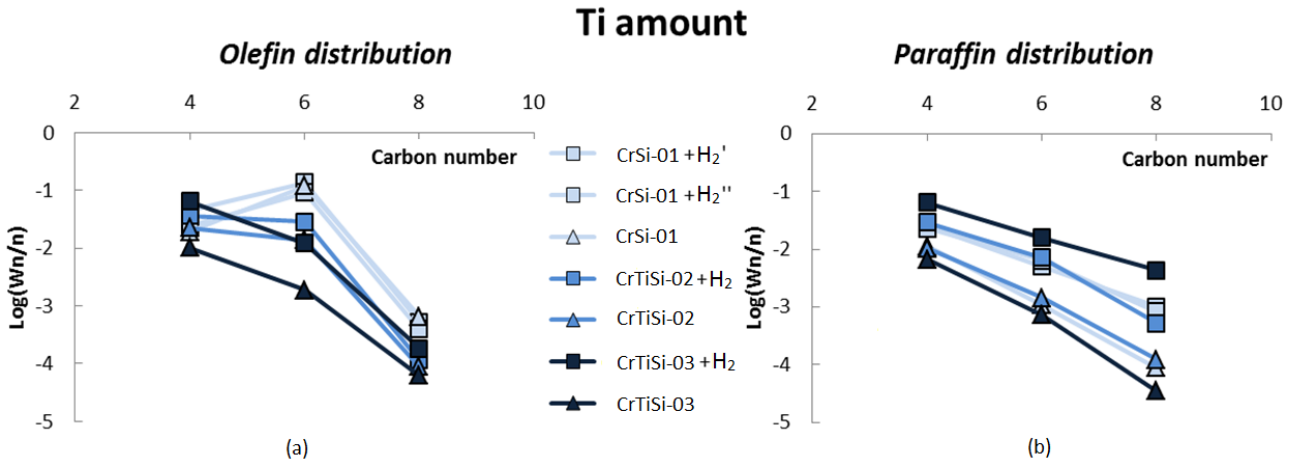

Figure 3.19: Catalysts with differing wt% Ti plotted according to the Schultz-Flory distribution.

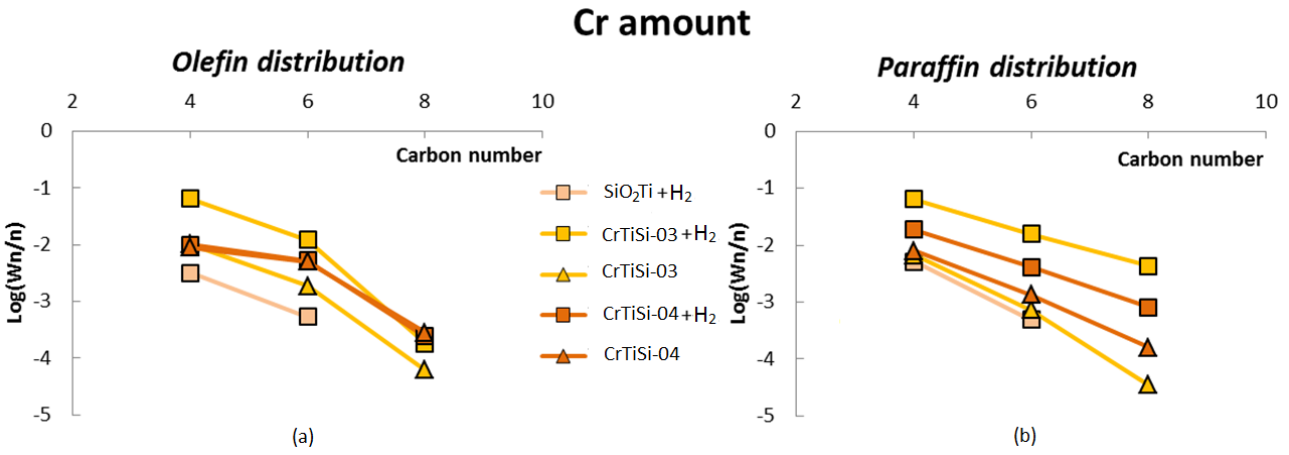

Figure 3.20: Catalysts with differing wt% Cr plotted according to the Schultz-Flory distribution.

Mechanisms

As mentioned before in the introduction, it is believed that the mechanism for the polymerization over the Phillips catalyst goes most likely via the Cossee-Arlman (linear insertion) mechanism (Figure 1.4(a)). [22] This is the mechanism that follows the ASF linear insertion distribution. However, from our results described above, there is another mechanism responsible for the oligomerization of the lower olefins. The metallacycle mechanism, mentioned in the introduction, can explain the olefin formation. A detailed schematic representation of this mechanism is given in Figure 3.21. The metallacycle mechanism does not need the addition of H_2 into the reaction mixture, which is necessary with the Cossee-Arlman mechanism. This could be an explanation for when no H_2 is added into the reaction mixture, there is an selectivity towards the forming of unsaturated hydrocarbons, *i.e.* olefins. The presence or absence of Ti might also be of great importance for this mechanistic route, since Ti influences the electronic structure of the active catalyst as explained in Section 3.2. This is causing a selectivity towards a certain olefin and it can either terminate the ring and release the oligomer or react further with another ethylene monomer and increase its size.

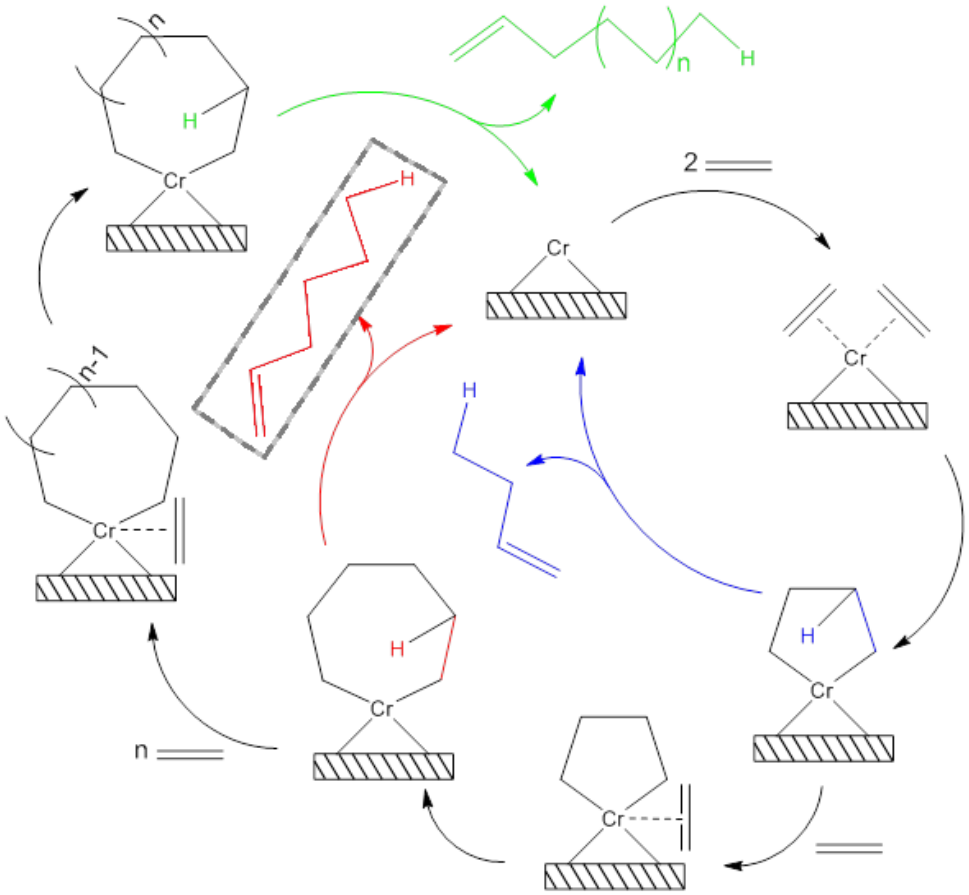

Figure 3.21: Detailed schematic representation of the metallacylce mechanism responsible for the oligomerization of ethylene. The striped rectangle represents the desired product, 1-hexene.

Chapter 4

Conclusions

In this thesis the oligomerization and polymerization of ethylene over a SiO_2-supported chromium catalyst have been investigated. More specific, the oligomerization of ethylene *in-situ* to 1-hexene and its co-polymerization into LLDPE were the main goals for this research in order to elucidate the exact nature of oligomerization species and the mechanism behind the reaction. In order to get more insight different characterization techniques have been utilized. These techniques include *in-situ* Diffuse Reflectance Fourier Transform Infrared Spectroscopy (DRIFTS), UV-Visible Near Infrared Diffuse Reflectance Spectroscopy (UV-Vis-NIR DRS) and Gas Chromatography-Mass Spectrometry (GC-MS).

4.1 *In-situ* DRIFT Spectroscopy

With the DRIFTS experiments no *in-situ* produced olefins could be detected due to the overlap of the vibrations with ethylene. It is also seen that the promoting effect of the TEAl co-catalyst is high. TEAl extremely promotes the polymerization of ethylene by reducing, modifying and alkylating the catalyst and also scavenging off poison of the highly sensitive polymerization reaction.

Furthermore, from Figures 3.1 and 3.2 it can be deduced that there are no noticeable differences in the IR spectra due to the added H_2. However, the effect of H_2 becomes more clear from the analysis of the sampled gas for the GC-MS experiments.

Transmission FT-IR Spectroscopy

From the Transmission FT-IR Spectroscopy it was clear that the formed polymer did not have a defined crystalline structure as shown by the intensity ratio of the two bands at 729 and 718 cm^{-1}. This lack of crystallinity could be an indication of branching within the polymer chains by *in-situ* formed olefins. Which were then copolymerized with ethylene to form branched type of PE of reduced crystallinity.

4.2 *In-situ* UV-Vis-NIR Diffuse Reflectance Spectroscopy

In-situ UV-Vis-NIR DRS experiments were performed in order to get more insight into the electronic changes within the catalyst and vibrational changes within the forming polymer during the reaction. From Figures 3.6-3.9 it can be deduced that H_2 plays a role in the reduction of the catalysts.

Furthermore, it is observed that with different Ti loading present in the catalysts, the three bands belonging to $O \rightarrow Cr^{6+}$ CT shift towards lower wavenumbers when the amount of Ti is increased. This is due to the electronic effect which Ti has on the active sites of the catalyst.

4.3 GC-MS

GC-MS analysis was performed on the sampled gas from both the DRIFTS and the UV-Vis-NIR DRS experiments. On the latter one, GC was performed as well in order to separate and detect the lower olefins formed and quantify results.

4.3.1 GC-MS from the DRIFTS Experiments

From the analysis of the sampled gas from the DRIFTS experiments in can be concluded that TEAl is extremely promoting the reaction. With GC-MS olefins could be detected and assigned with 1-hexene as the main C6 fraction. However, some higher olefins (octenes, decenes and dodecenes) were detected as well. When H_2 is added into the gas composition more hexanes are produced. Therefore, H_2 also plays a role in the hydrogenation of alkenes into alkanes. With the combination of GC-MS it was not possible to detect the C4 fraction. This fraction has a retention time that is too short to be separated from the ethylene reactant.

4.3.2 GC-MS from the UV-Vis-NIR DRS Experiments

For the analysis of the sampled gas of the UV-Vis-NIR DRS experiments, GC-MS and only GC analysis were performed. This way, lower olefin fractions could be detected. From Section 3.4.2 it can be seen that both H_2 and Ti have important influences on the oligomerization and polymerization of ethylene.

H_2 increases the overall hydrocarbon yield. It also decreases the selectivity towards olefins and increases the selectivity towards paraffins. Increasing the amount of Ti loading decreases the overall hydrocarbon productivity. Furthermore, increasing the Ti loading lowers the selectivity towards olefins, while increasing the selectivity towards paraffins.

From all this, it is also clear that there are two different mechanism responsible for the formation of polymers and olefins. The Cossee-Arlman, linear insertion, should be responsible for the polymerization of ethylene and the metallacycle is most probably responsible for the oligomerization of ethylene.

4.3.3 Summary

Ethylene was successfully oligomerized *in-situ* in the DRIFTS and UV-Vis-NIR DRS cell, which was detected by GC-MS and GC, with 1-hexene as the main C6 fraction formed. The TEAL co-catalyst highly promotes polymerization and oligomerization. H_2 reduces the catalyst and leads to less olefins being formed. Increase of Ti loading causes a decrease of olefin selectivity. Furthermore, two different mechanisms are responsible for the polymerization and oligomerization, Cossee-Arlman and metallacycle respectively.

4.3.4 Outlook

For future experiments, measurements with deuterated ethylene and deuterium gas should be done in order to identify the role of H_2. Does the H_2 incorporate in the polyethylene chains or is it incorporated into the oligomers. DRIFTS and UV-Vis-NIR DRS with online MS should also be performed. With this combination we would be able to detect the different products formed at the different times. Furthermore, DRIFTS and UV-Vis-NIR DRS experiments under higher pressures (*i.e.*, 10 bar), should be performed in order to get closer to industrial conditions. And last but not least, experiments with catalyst with different Ti distributions, shell and/or bulk, should be performed in order to identify the role of Ti. [35]

Appendix A

Experimental Approach

For the characterization of the catalysts and the oligo/polymerization reaction several techniques were used, including Infrared Spectroscopy (IR), Gas Chromatography - Mass Spectrometry (GC-MS), Low Resolution Scanning Microscopy (SEM) and Ultraviolet-Visible Near-Infrared Diffuse Reflectance Spectroscopy (UV-Vis-NIR DRS).

A.1 Infrared Spectroscopy

IR spectroscopy is a technique that deals with the infrared region of the electromagnetic spectrum and is the most common form of vibrational spectroscopy. The IR part of the electromagnetic spectrum ranges from wavelengths of 1 mm (300 GHz) to 750 nm (400 THz) and can be divided into three different regions:

- Far-IR, from 1 mm to 10 μm
- Mid-IR, from 10 to 2.5 μm
- Near-IR, from 2.5 μm to 750 nm

There are several different IR spectroscopy techniques, *e.g.* transmission, diffuse reflection, emission and Raman scattering. The former two are going to be discussed in the next sections. All techniques make use of the fact that molecules absorb electromagnetic radiation of specific energies (hν) if the energy of the radiation matches the transition energy of the bond or group that vibrates. These energies are determined by the properties of the molecules, like strength of the bond and mass of the atoms.

A molecule can vibrate in numerous ways which are called vibrational modes. The number of different vibrational modes that a molecule or a group possesses can be determinded from the following considerations. A molecule consisting of N atoms has 3N degrees of freedom. Three of these are translational degrees of freedom of the molecule and three are rotations of the molecule along the three principal axes of inertia. Linear molecules have only two rotational degrees of freedom, as no energy change is involved in the rotation along the main axis. Thus, the number of fundamental vibrations is 3N-6 for a non-linear and 3N-5 for a linear molecule. [36]

There are four types of vibrations (Figure A.1):

- Stretching vibrations (ν), changing the length of a bond.
- Bending vibrations in one plane (δ), changing bond angles but leaving bond lenghts unaltered (in larger molecules further divided into rock, twist and wag vibrations).
- Bending vibrations out of plane (γ), in which one atom oscillates through a plane defined by at least three neighboring atoms.
- Torsion vibrations (τ), changing the angle between two planes through atoms.

Absorption of an infrared photon occurs only if a dipole moment changes sufficiently during the vibration, so not all vibrations can be observed. The intensity of the infrared band is proportional to

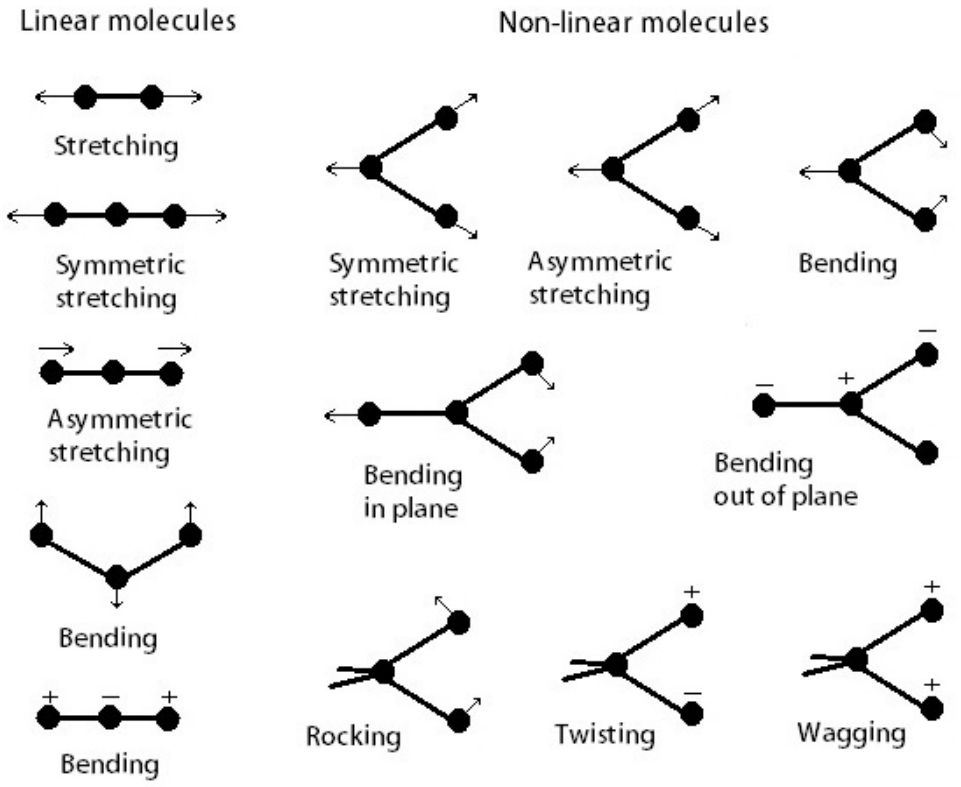

Figure A.1: Fundamental vibrations of several model molecules. [36]

the change in dipole moment.

With the assumption of a linear harmonic oscillator, the energy and frequency of the absorbed IR radiation can be given as (Equations A.1, A.2 and A.3):

$$E_n = (n + \frac{1}{2})h\nu \tag{A.1}$$

$$\nu = \frac{1}{2\pi}\sqrt{\frac{k}{\mu}} \tag{A.2}$$

$$\frac{1}{\mu} = \frac{1}{m_1} + \frac{1}{m_2} \text{ or } \mu = \frac{m_1 m_2}{m_1 + m_2} \tag{A.3}$$

where:
n is the vibrational quantum number;
h is Planck's constant;
ν is the frequency;
k is the spring constant for the bond;
c is the speed of light;
μ is the reduced mass of the 1-2 system ($m_\#$ is the mass of atom $_\#$).

A.1.1 Transmission Fourier Transfer-Infrared Spectroscopy

Transmission Fourier Transfer Infrared Spectroscopy (FT-IR) is the most common form of IR spectroscopy. The infrared radiation of the sample is detected after it is transmitted through a pellet. The pellet most commonly consists of the tested sample with KBr powder, which is optional to dilute

the sample if the signal of tested sample alone is too strong, pressed into a self-supporting pellet of approximately 1 cm^2 and a few tenths of a millimeter thickness. [36] When the infrared radiation is transmitted through the pellet a molecular fingerprint is made, which provides information about the composition of the material, *i.e.* what kind of bonds are present in the material. FT-IR provides a very simple way of measuring such data. However, no *in-situ* experiments can be performed with this technique.

A.1.2 Diffuse Reflection Infrared Fourier Transform Spectroscopy

Diffuse Reflection Infrared Fourier Transform Spectroscopy (DRIFTS) is an important tool for the characterization of the surface reactivity of gas sensing materials under reactive atmosphere. DRIFTS analysis of powders is conducted by focusing infrared light onto the powder (sometimes diluted in a non absorbing matrix, like KBr) and the scattered light is collected and relayed to the IR detector.

There are different kinds of infrared radiation, as illustrated in Figure A.2. When infrared radiation is directly reflected from the sample surface, it gives rise to specular refraction, which is a function of the refractive index and absorptivity of the sample. The radiation may also undergo multiple reflections between the particles without penetrating the particle themselves. The radiation that exits the surface than, has any angle relatively to the incident beam and can be called diffuse specular reflection. These kind of diffuse specular reflection does not contain any information about the sample. True diffusion reflection is the consequence of beam penetration into one or more particles and its diffusion in the sample. [37] These reflections also exit the surface at any angle however, since they have traveled through the particles, they contain data on the absorption properties of the material. Because of these properties, diffuse radiation contains similar information about the material as transmission radiation.

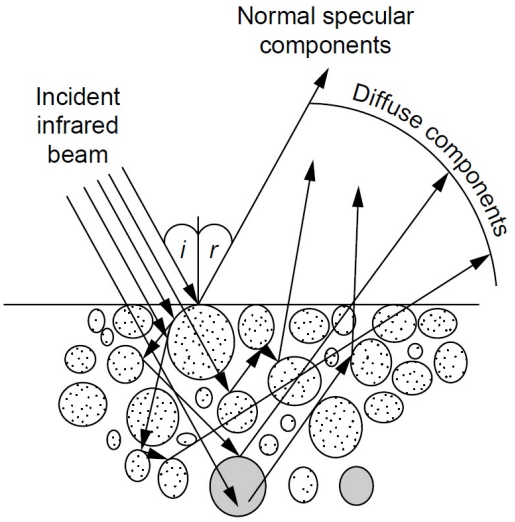

Figure A.2: Schematic representation of generating the infrared spectrum of a powder. [37]

The different radiations can not be optically separated, but if the specular diffuse reflection component is weak compared with diffuse reflection than the spectra are quite similar to transmission spectra. Refractive index of the sample, particle dimensions, packing density, homogeneity, concentration and absorption coefficients all have influences on the quality of the DRIFTS spectrum as well.

The main advantages of this technique reside in the ease of sample preparation and the ability to analyze nontransparent materials, which could not be analyzed by transmission IR spectroscopy. Besides, since the spectra are recorded *in-situ*, one can 'see' the catalyst working by monitoring the changes of species on its surface.

This technique not only permits the analysis at atmospheric pressure but also under increased pressure, suggesting the use of DRIFTS spectroscopy as a tool for characterization designed for work on catalysts in conditions very similar to those encountered during a catalytic action. [37]

A.2 UV-Vis-NIR Diffuse Reflectance Spectroscopy

Ultraviolet-Visible Near-Infrared Diffuse Reflectance Spectroscopy (UV-Vis-NIR DRS) is a valuable technique for the characterization of catalysts and is based on measurements of both electronic (UV-Vis) and vibrational (NIR) transitions. [38] It is a nondestructive method for analyzing samples of various physical states, shapes and thickness *in-situ*. Therefore, UV-Vis-NIR spectroscopy can be used for the in- and online process monitoring of chemical and physical properties of the material, [32] *i.e.* providing information about coordination, oxidation states of the metal and charge transfer transitions. The principle of UV-Vis-NIR DRS is the same as the infrared spectroscopy described above (use of diffuse components of the radiation, as in Figure A.2) , however it uses different energies to excite the samples, *i.e.* UV-Vis and NIR region of the electromagnetic spectrum.

Althought the technique behind DRS is the same as, for example, with FT-IR, the diffuse reflectance spectra will appear different from its transmission equivalent, *i.e.* stronger than expected absorption from weak IR bands. [39] To compensate for these difference, the spectra are often converted via the Kulbelka-Munk (K-M) function, a simplified analysis of the interaction of incoming light with the sample. Before using the K-M function one has to take a few assumptions into account:

1. An infinite layer thickness;
2. A low concentration of absorbing centers;
3. A uniform distribution of absorbing centers;
4. Diffuse monochromatic irradiation of the powdered sample;
5. The absence of fluorescence
6. Isotropic light scattering.

In such system, the following form of the K-M equation can be applied (Equation A.4): [39, 40]

$$F(R) = \frac{(1 - R_\infty)^2}{2R_\infty} = \frac{k}{s} \tag{A.4}$$

where:
R_∞ is the absolute reflectance of the sample divided by a standard (absolutely white reference);
k is the molar absorption coefficient;
s is the scattering coefficient.

A.3 Chromatography

Chromatography is the technique of separating and analyzing the components of a mixture of liquids or gases by selective adsorption in, *i.e.* a column of powder (column chromatography) or on a strip of paper (paper chromatography). [41]

In chromatography, one phase is held stationary while another phase moves past it. If a solution of two solvents A and B is placed on top of a column, as illustrated in Figure A.3, solutes, A and B,

flow down into the column when the outlet is opened. Fresh solvent is then applied to the top of the column and the mixture is washed down the column by continuous solvent flow. If solute A is more strongly adsorbed than solute B on the solid particles, then solute A spends a smaller fraction of the time free in the solution. Solute A moves down the column more slowly than solute B and emerges at the bottom after solute B. [42]

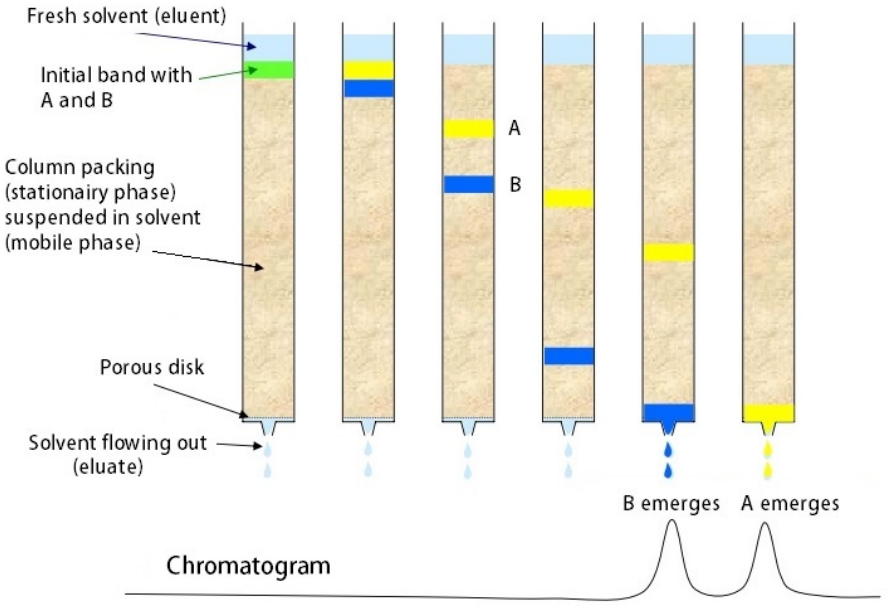

Figure A.3: The principle of chromatography: Solute A, with a greater affinity than solute B for the stationary phase, remains on the column longer. [42]

The time needed for each component to reach the detector after injection of the mixture is called the **retention time**, t_r. Retention volume, V_r, is the volume of mobile phase required to elute a particular solute from the column. Unretained mobile phase travels through the column in the minimum possible time, designated t_m. The **adjusted retention time**, $t_r^{'}$, for a solute is the additional time required for solute to travel the length of the column beyond the time required by unretained solvent: [42]

$$t_r^{'} = t_r - t_m \tag{A.5}$$

In gas chromatography, t_m is usually taken as the time needed for CH_4 to travel through the column. The separation between two components can be measured in relative retention. For any two components A and B, the **relative retention**, α, is the ratio of their adjusted retention times:

$$\alpha = \frac{t_{rB}^{'}}{t_{rA}^{'}} \tag{A.6}$$

where $t_{rB}^{'} > t_{rA}^{'}$, so $\alpha > 1$. The relative retention can help to identify peaks because it is independent of flow rate. The adjusted retention time can help to monitor the performance of the column in the form of the **capacity factor**. The longer a component is retained by the column, the greater is the capacity factor:

$$k^{'} = \frac{t_r - t_m}{t_m} \tag{A.7}$$

Two factors play a important role in how well components are separated by chromatography. The first is the elution time of the components/peaks. The further apart, the better the separation. The second factor is the width of the peaks. The broader the peaks, the poorer their separation. The latter can be expressed by the resolution and is defined by:

$$Resolution = \frac{\Delta t_r}{w_{av}} = \frac{\Delta V_r}{w_{av}} \tag{A.8}$$

where Δt_r or ΔV_r is the separation between the peaks and w_{av} is the average width of the two peaks (measured at the bottom). Solute moving through a chromatography column tends to spread into a Gaussian shape with standard deviation σ. The longer the solute spends in the column, the broader the band becomes. Figure A.4 illustrates the basic concept of resolution.

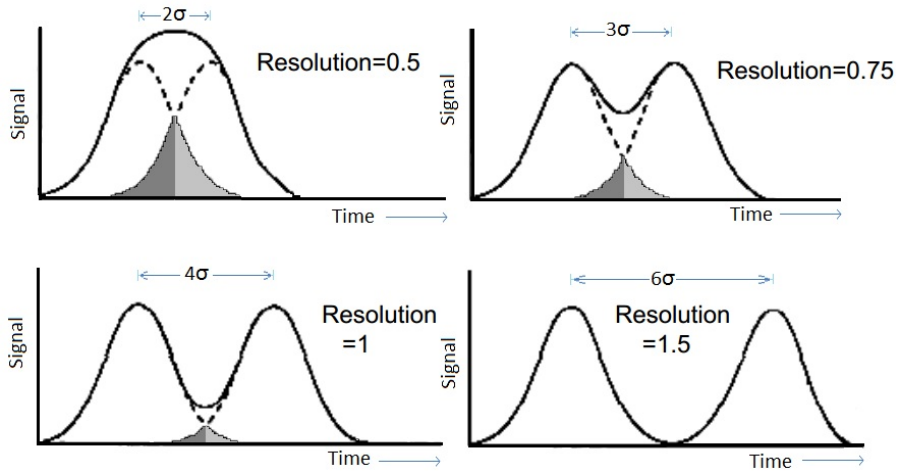

Figure A.4: Resolution of Gaussian peaks of equal area and amplitude. [42]

A.3.1 Gas Chromatography

In Gas Chromatography (GC), a volatile liquid or gaseous solute is carried over a stationary phase on the inside of a column or on a solid support by a gaseous mobile phase, called the carrier gas. A schematic diagram of a gas chromatograph is represented by Figure A.5.

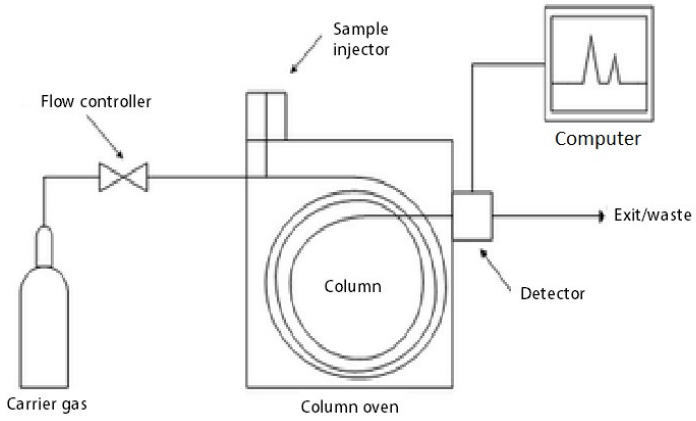

Figure A.5: Schematic diagram of a gas chromatograph. [42]

Volatile liquid or gaseous sample is injected through a septum into a heated port, in which it rapidly evaporates. The vapor is carried further into the column by the carrier gas (which must be dry, free of oxygen and chemically inert, like H_2, N_2 or He). The separated solutes flow through the detector and are displayed on a computer in a chromatograph. It is important that the temperature

of the detector is higher than the temperature of the column so all solutes will be gaseous. The carrier gas plays an important role in, for example, analysis time, elution temperature and sensitivity. Which gas is used and what particular role it plays depends also on the detector used. [43]

There are open tubular columns and packed columns. The first are the most common and are made of fused silica (SiO_2) and coated with polyimide (a plastic capable of withstanding 350 °C) for support and protection from atmospheric moisture. The latter are made of glass or a metal tubing and contain densely packed fine particles of solid support coated with nonvolatile liquid stationary phase, or the solid itself may be the stationary phase. When comparing these two columns, open tubular columns offer higher resolution, shorter analysis time, greater sensitivity and lower sample capacity. [42]

Temperature plays an important role in the retention time of the solutes. Raising the temperature of a column decreases the retention time and sharpens the peaks. With a temperature program one can control when compounds emerges from the column. Where some less volatile compounds may not even be eluted from the column at a certain temperature, the temperature can be raised in order to let them emerge. When compounds emerge from the column close together, it is sometimes also necessary to use a temperature program in order to separate the peaks more. Pressure can also be used to decrease the retention time of the solutes. In principle it works the same way as temperature programming however, at the end of the run the pressure can be rapidly reduced to its initial value for the next run. While temperature programming first needs to cool down before the next injection.

A.4 Mass Spectrometry

Mass Spectrometry (MS) is a technique for studying the masses of atoms, molecules or fragments of molecules. It uses ionized species from a gaseous phase to obtain a spectrum. The ions are accelerated by an electric field and then separated according to their mass-to-charge ratio, m/z, [42] where m refers to the molecular or atomic mass number and z to the charge number of the ion. This makes m/z a dimensionless quantity. If all charges are +1, then m/z is equal to the mass. If an ion has a charge of +2, then m/z is half of the mass.

Although there are various MS instruments, all have three essential components (Figure A.6). The first common component is the ionization source. Here, the molecules are given a positive electrical charge by removing an electron or adding a proton. Electrons emitted from a hot filament are accelerated through 70 V before interacting with the incoming molecules. A small amount ($\approx 0.01\%$) of the molecules absorb as much as 12-15 electron volts (1 eV = 96.5 kJ/mol), which is enough for ionization: [42]

$$M + \underset{70\text{ eV}}{e^-} \rightarrow \underset{\text{Molecular ion}}{M^{+\bullet}} + \underset{\approx 55\text{ eV}}{e^-} + \underset{0.1\text{ eV}}{e^-} \tag{A.9}$$

Depending on the ionization method used, the ionized molecules may or may not break down into a population of smaller fragments. Among these fragments there are positively charged fragments and neutral fragments. The latter ones are either absorbed onto the walls of the chamber or are removed by a vacuum source. [44]

The second essential component of the MS instrument is the mass analyzer. Here the cationic fragments and remaining unfragmented molecular ions are separated according to their mass. In Figure A.7 it is illustrated how this in principle works. The ionized fragments are accelerated by an electric field and deflected in a curved tube by a strong magnetic field. The deflection of the ions is depended on their mass, resulting in a sorting of the ions. Most of the ions will have charges of z = +1, which makes sorting by the mass-to-charge ratio the same as sorting by mass.

At the end of the curved tube there is the third essential component of the MS instrument, the detector. Here are the sorted ions recorded and quantified.

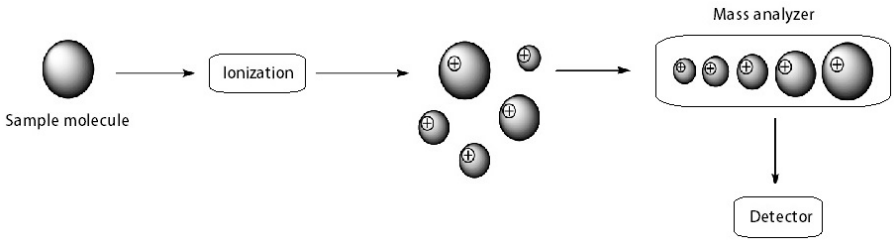

Figure A.6: Simplified illustration of a mass spectrometer. [44]

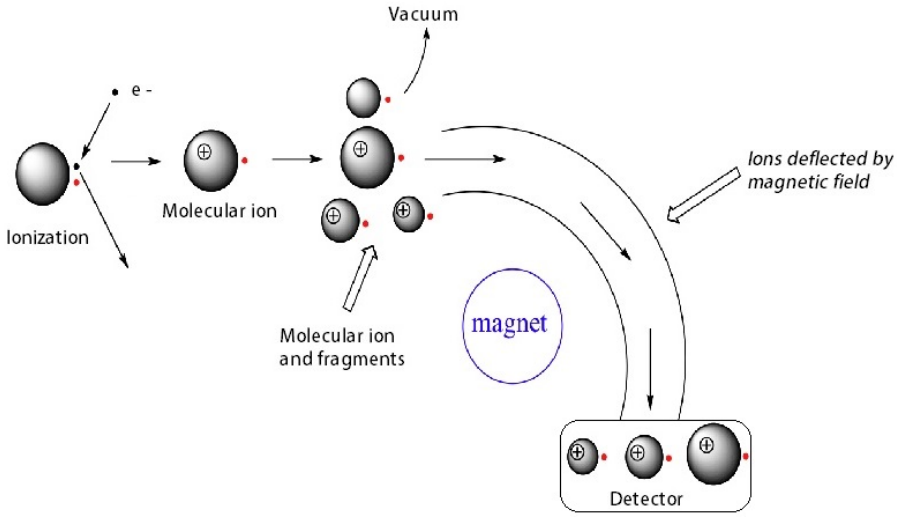

Figure A.7: The mass analyzer. [44]

A.5 Gas Chromatography-Mass Spectrometry

Gas Chromatography and Mass Spectrometry (GC-MS) is a very powerful combination for analyzing volatile liquids or gaseous mixtures. Where the gas chromatograph separates the components in the mixture, the mass spectrometer can identify these peaks by creating mass spectra and compare them with a library of known spectra. GC-MS is build up by a gas chromatograph and a mass spectrometer at the outlet of the GC acting as a detector, as illustrated in Figure A.8.

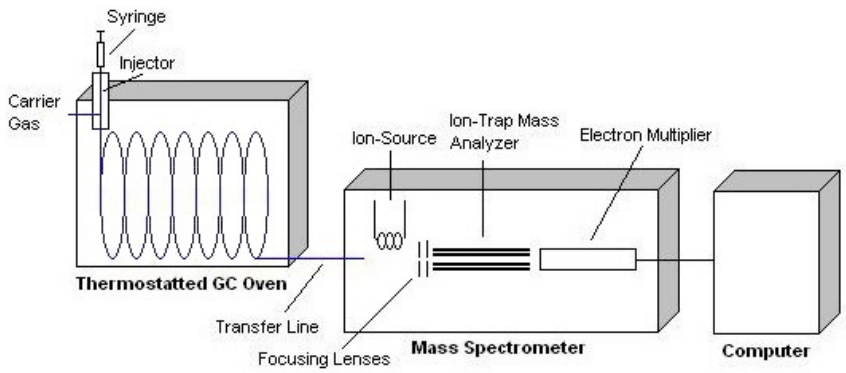

Figure A.8: Schematic representation of the GC-MS system. [43]

Bibliography

[1] W. Reusch, "Different Polymers, https://www.chemistry.msu.edu," 2013, *accessed* : 12-12-2013.

[2] E. Groppo, C. Lamberti, S. Bordiga, G. Spoto, and A. Zecchina, "The Structure of Active Centers and the Ethylene Polymerization Mechanism on the Cr/SiO_2 Catalyst: a Frontier for the Characterization Methods.," *Chemical Reviews*, vol. 105, pp. 115–184, 2005.

[3] The University of York, "Polyethylene, http://www.essentialchemicalindustry.org," 2014, *accessed* : 23-01-2014.

[4] S. Likhitlert, C. Wongchaleo, A. Kositchaiyong, E. Wimolmala, S. Mitrprasertporn, and N. Sombatsompop, "Thermal Characteristics and Temperature Profile Changes of Structurally Different Polyethylenes With Peroxide Modifications," *Journal of Vinyl and Additive Technology*, vol. 20, pp. 80–90, 2014.

[5] B. M. Weckhuysen and R. A. Schoonheydt, "Olefin Polymerization Over Supported Chromium Oxide Catalysts," *Catalysis Today*, vol. 51, pp. 215–221, 1999.

[6] L. Wang, B. Yang, B. Yin, N. Sun, J.-M. Feng, and M.-B. Yang, "Thermorheology and Crystallization Behaviors of Polyethylenes: Effect of Molecular Attributes," *Journal of Macromolecular Science, Part B*, vol. 52, pp. 1479–1493, 2013.

[7] M. P. McDaniel, "A Review of the Phillips Supported Chromium Catalyst and its Commercial Use for Ethylene Polymerization," *Advances in Catalysis*, vol. 53, pp. 123–606, 2010.

[8] J. P. Hogan and R. L. Banks, "U.S. Patent 2,825,721," 1958.

[9] K. Ziegler, "Belgian Patent 533,362," 1954.

[10] B. M. Weckhuysen, I. E. Wachs, and R. A. Schoonheydt, "Surface Chemistry and Spectroscopy of Chromium in Inorganic Oxides.," *Chemical Reviews*, vol. 96, pp. 3327–3350, 1996.

[11] A. Zecchina and E. G. A. Damin, "Anatomy of Catalytic Centers in Phillips Ethylene Polymerization Catalyst," *Topics in Organometallic Chemistry*, vol. 16, pp. 1–35, 2005.

[12] E. Groppo, K. Seenivasan, and C. Barzan, "The Potential of Spectroscopic Methods Applied to Heterogeneous Catalysts for Olefin Polymerization," *Catalysis Science and Technology*, vol. 3, pp. 858–878, 2013.

[13] W. Kaminsky, "Discovery of Methylaluminoxane as Cocatalyst for Olefin Polymerization," *American Chemical Society*, vol. 45, pp. 3289–3297, 2012.

[14] H. S. Cho, J. S. Chung, and W. Y. Lee, "Control of Molecular Weight Distribution for Polyethylene Catalyzed over ZieglerNatta/Metallocene Hybrid and Mixed Catalysts," *Journal of Molecular Catalysis A: Chemical*, vol. 159, pp. 203–213, 2000.

[15] M. Atiqullah, S. Anantawaraskul, A.-H. M. Emwas, M. A. Al-Harthi, I. Hussain, A. Ul-Hamid, and A. Hossaen, "Silica-Supported (n-BuCp) 2-$ZrCl_2$: Effect of Catalyst Active Center Distribution on Ethylene-1-Hexene Copolymerization," *Polymer International*, vol. 63, pp. 955–972, 2014.

[16] M. McDaniel, "Supported Chromium Catalysts for Ethylene Polymerization," *Advances in Catalysis*, vol. 33, pp. 47–98, 1985.

[17] C. Barzan, E. Groppo, E. A. Quadrelli, V. Monteil, and S. Bordiga, "Ethylene Polymerization on a SiH_4-Modified Phillips Catalyst: Detection of *In-Situ* Produced α-Olefins by Operando FT-IR Spectroscopy," *Physical Chemistry Chemical Physics*, vol. 14, pp. 2239–2245, 2012.

[18] Sigma-Aldrich Co. LLC., "Sigma-Aldrich, www.sigma-aldrich.com," 2015, *accessed* : 21-01-2015.

[19] A. Budnyk, A. Damin, C. Barzan, E. Groppo, C. Lamberti, S. Bordiga, and A. Zecchina, "Cr-Doped Porous Silica Glass as a Model Material to Describe Phillips Catalyst Properties," *Journal of Catalysis*, vol. 308, pp. 319–327, 2013.

[20] A. Zecchina and E. Groppo, "Surface Chromium Single Sites: Open Problems and Recent Advances," *Proceedings of the Royal Society A: Mathematical, Physical and Engineering Sciences*, vol. 468, pp. 2087–2098, 2012.

[21] E. Groppo, C. Lamberti, S. Bordiga, G. Spoto, and A. Zecchina, "*In-Situ* FTIR Spectroscopy of Key Intermediates in the First Stages of Ethylene Polymerization on the Cr/SiO_2 Phillips Catalyst: Solving the Puzzle of the Initiation Mechanism?," *Journal of Catalysis*, vol. 240, pp. 172–181, 2006.

[22] D. S. McGuinness, N. W. Davies, J. Horne, and I. Ivanov, "Unraveling the Mechanism of Polymerization With the Phillips Catalyst," *Organometallics*, vol. 29, pp. 6111–6116, 2010.

[23] R. Cheng, Z. Liu, L. Zhong, X. He, P. Qiu, M. Terano, M. S. Eisen, S. L. Scott, and B. Liu, "Phillips Cr/Silica Catalyst for Ethylene Polymerization," *Advances in Polymer Science*, vol. 275, pp. 135–202, 2013.

[24] E. Groppo, A. Zecchina, C. Barzan, and J. G. Vitillo, "Low Temperature Activation and Reactivity of CO_2 Over a Cr(II)-Based Heterogeneous Catalyst: a Spectroscopic Study," *Physical Chemistry Chemical Physics*, vol. 14, pp. 6538–6543, 2012.

[25] W. Xia, K. Tonosaki, T. Taniike, M. Terano, T. Fujitani, and B. Liu, "Copolymerization of Ethylene and Cyclopentene With the Phillips CrO_x/SiO_2 Catalyst in the Presence of an Aluminum Alkyl Cocatalyst," *Journal of Applied Polymer Science*, vol. 111, pp. 1869–1877, 2008.

[26] E. Groppo, J. Estephane, C. Lamberti, G. Spoto, and A. Zecchina, "Ethylene, Propylene and Ethylene Oxide *In-Situ* Polymerization on the $Cr(II)/SiO_2$ System: A Temperature- and Pressure-Dependent Investigation," *Catalysis Today*, vol. 126, pp. 228–234, 2007.

[27] E. Groppo, C. Lamberti, S. Bordiga, G. Spoto, A. Damin, and A. Zecchina, "FT-IR Investigation of the H_2, N_2, and C_2H_4 Molecular Complexes Formed on the Cr(II) Sites in the Phillips Catalyst: a Preliminary Step in the Understanding of a Complex System," *Journal of Physical Chemisty B*, vol. 109, pp. 15024–15031, 2005.

[28] S. Bordiga, S. Bertarione, A. Damin, C. Prestipino, G. Spoto, C. Lamberti, and A. Zecchina, "On the First Stages of the Ethylene Polymerization on Cr^{2+}/SiO_2 Phillips Catalyst: Time and Temperature Resolved IR Studies," *Journal of Molecular Catalysis A: Chemical*, vol. 204-205, pp. 527–534, 2003.

[29] A. D. McNaught and A. Wilkinson, *IUPAC. Compendium of Chemical Terminology*, p. 359. Blackwell Scientific Publications, Oxford, 2nd ed., 2007.

[30] M. F. Delley, M. P. Conley, and C. Copéret, "Polymerization on CO-Reduced Phillips Catalyst Initiates Through the CH Bond Activation of Ethylene on CrO Sites," *Catalysis Letters*, vol. 144, pp. 805–808, 2014.

[31] W. Jozwiak, "On the Role of Surface Hydroxyls During the Cr/SiO_2-Catalyzed Polymerization of Ethylene," *Journal of Catalysis*, vol. 121, pp. 183–195, 1990.

[32] M. Watari, "A Review of Online Real-Time Process Analyses of Melt-State Polymer Using the Near-Infrared Spectroscopy and Chemometrics," *Applied Spectroscopy Reviews*, vol. 49, pp. 462–491, 2013.

[33] B. M. Weckhuysen, R. R. Rao, J. Pelgrims, R. A. Schoonheydt, P. Bodart, G. Debras, O. Collart, P. V. D. Voort, and E. F. Vansant, "Synthesis, Spectroscopy and Catalysis of [$Cr(acac)_3$] Complexes Grafted onto MCM-41 Materials : Formation of Polyethylene Nanofibres Within Mesoporous Crystalline Aluminosilicates," *Chemistry: A European Journal*, vol. 6, pp. 2960–2970, 2000.

[34] R. W. Dorner, D. R. Hardy, F. W. Williams, and H. D. Willauer, "Heterogeneous Catalytic CO_2 Conversion to Value-Added Hydrocarbons," *Energy And Environmental Science*, vol. 3, pp. 884–890, 2010.

[35] D. Cicmil, H. E. van der Bij, I. K. van Ravenhorst, J. Wang, J. Meeuwissen, A. Vantomme, and B. M. Weckhuysen - *In preparation*.

[36] J. W. Niemantsverdriet, *Spectroscopy in Catalysis*, ch. 8, pp. 217–247. Wiley-VCH, Weinheim, 3rd ed., 2007.

[37] T. Armaroli, T. Bécue, and S. Gautier, "Diffuse Reflection Infrared Spectroscopy (Drifts): Application to the *In-Situ* Analysis of Catalysts," *Oil and Gas Science and Technology*, vol. 59, pp. 215–237, 2004.

[38] F. C. Jentoft, "Ultraviolet-Visible-Near Infrared Spectroscopy in Catalysis: Theory, Experiment, Analysis, and Application Under Reaction Conditions," *Advances in Catalysis*, vol. 52, pp. 129–211, 2009.

[39] A. Escobedo Morales, E. Sánchez Mora, and U. Pal, "Use of Diffuse Reflectance Spectroscopy for Optical Characterization of Un-Supported Nanostructures," *Revista Mexicana de Física S*, vol. 53, pp. 18–22, 2007.

[40] B. M. Weckhuysen, *In Situ Spectroscopy of Catalysts*, ch. 12, pp. 255–270. American Scientific Publishers, 1st ed., 2004.

[41] The Free Dictionairy by Farlex, "Chromatography, http://www.thefreedictionary.com/," 2014, *accessed* : 09-04-2014.

[42] D. C. Harris, *Quantitative Chemical Analysis*, ch. 22, pp. 474–495. W. H. Freeman and Company, New York, 7th ed., 2007.

[43] Chemwiki, UCDavis, "Gas Chromatography, http://chemwiki.ucdavis.edu," 2014, *accessed* : 10-04-2014.

[44] Chemwiki, UCDavis, "Mass Spectrometry, http://chemwiki.ucdavis.edu," 2014, *accessed* : 10-04-2014.